DEVELOPMENT OF A ROBUST METHODOLOGY TO OBTAIN AND ASSESS

MYOGENIC PRECURSOR CELLS FOR THEIR USE IN REGENERATIVE

THERAPIES

A Thesis

presented to

the Faculty of California Polytechnic State University,

San Luis Obispo

In Partial Fulfillment

of the Requirements for the Degree

Master of Science in Biomedical Engineering

by

Ricardo Lasa Rivas

March 2021

COMMITTEE MEMBERSHIP

TITLE: Development of a Robust Methodology to
Obtain and Assess Myogenic Precursor Cells
for Their Use in Regenerative Therapies

AUTHOR: Ricardo Lasa Rivas

DATE SUBMITTED: March 2021

COMMITTEE CHAIR: Trevor Cardinal, Ph.D.
Professor of Biomedical Engineering

COMMITTEE MEMBER: Christopher Heylman, Ph. D.
Professor of Biomedical Engineering

COMMITTEE MEMBER: Lily Laiho, Ph. D.
Professor of Biomedical Engineering

# ABSTRACT

Development of a Robust Methodology to Obtain and Assess Myogenic Precursor Cells
for Their Use in Regenerative Therapies

Ricardo Lasa Rivas

Peripheral arterial occlusive disease (PAOD) is characterized by buildup of atherosclerotic plaque in peripheral arteries that leads to an occlusion that can interrupt the supply of blood to the peripheral tissue, causing downstream tissue ischemia/hypoxia. PAOD is estimated to affect over 200 million patients worldwide. Current surgical revascularization treatments can be effective in about half of the patient population, leading to a significant number of patients with no treatment options beyond pharmacological intervention and lifestyle modification. The decrease in blood flow downstream of the occlusion leads to increased blood pressure gradient in the microvasculature, specifically in vessels that connect arterial trees (known as collaterals), which will structurally enlarge and increase blood flow to the downstream ischemic/hypoxic tissue. Targeting this process, known as arteriogenesis, can provide a potential treatment option for patients suffering from PAOD by redirecting blood flow around an occluded artery and therefore supplying hypoxic tissue with blood. In order to enhance this process, cellular transplantation has been used but the current cell types explored have not been successful in enhancing arteriogenesis. Myoblasts, proliferative muscle progenitor cells, mediate muscle regeneration, and promote angiogenesis (the growth of new capillaries to supply hypoxic tissue). Preliminary data indicates that myoblasts also promote arteriogenesis in obese mice, making them an attractive therapeutic candidate. However, the methods used in the preliminary studies limited our ability to confirm those findings and characterize the cell therapy candidate. Specifically, we lacked a reproducible and optimized method to isolate myogenic cells and characterize these cells during in vitro culture and after in vivo transplantation. Therefore, the 1st Aim of this study was to optimize the isolation to obtain the highest number possible of satellite cell-yielding myofibers by modification of enzymatic and mechanical digestion of extensor digitorum longus muscle. Modifications to this methodology increased myofiber yield by more than 150%. The 2nd Aim was to optimize the expansion of satellite cell-derived myoblasts by modification of culture media supplements to promote cell expansion while minimizing maturation. bFGF and SB 203580 supplementation improved cell proliferation and prevented myogenic cell maturation during 7-days of in vitro culture. The 3rd Aim was to develop a process for evaluating the quantity and identity of isolated myogenic cells before and after transplantation. This was achieved by implementing an immunofluorescent transcription factor labeling protocol to determine cell identity and a live/dead cell viability assay to determine cell viability and quantity. All 3 aims were integrated into a proof-of-concept pilot study on a hindlimb ischemic BALB/c mouse model. While myoblast transplantation failed to increase collateral arteriogenesis in this model, the process developed in this project provides a reproducible framework for future studies on myoblast-enhanced arteriogenesis. Further research on the effects of myoblast transplantation on arteriogenesis may facilitate the development of new therapies that improve the prognosis of patients with PAOD.

Keywords: Cell therapy, myoblast, arteriogenesis, collateral, cell culture, PAOD

ACKNOWLEDGMENTS

"Somewhere, something incredible is waiting to be known"
- Carl Sagan

# TABLE OF CONTENTS

# LIST OF TABLES

LIST OF FIGURES

# 1. INTRODUCTION

Peripheral Arterial Occlusive Disease (PAOD) is characterized by the buildup of atherosclerotic

plaques on arterial walls, primarily in lower extremities (**Figure 1**)[1,2]. This leads to a narrowing of

arteries and reduction in blood flow to the affected area, resulting in ischemia. PAOD is estimated

to affect over 200 million individuals

worldwide[3]. Patients develop pain in the

affected extremities that can lead to

functional impairment (intermittent

claudication), which is the most common

symptom of PAOD[3,4]. In more severe

cases, ischemia can also lead to gangrene

and subsequent amputation[3–5].

Treatments for PAOD revolve around the

reduction of risk factors for

atherosclerosis, such as lifestyle

modifications or pharmacological



Figure 1: Peripheral Arterial Occlusive Disease. Narrowing of artery due to plaque buildup reduces blood flow supply to extremities.

management of blood pressure and clot formation (antiplatelet drugs can be administered to

patients to decrease the likelihood of clot formation but do not serve as a therapy for reducing

PAOD)[1,3,6]. Surgical revascularization procedures (such as bypass grafts) or more modern

endovascular revascularization strategies (angioplasty) are employed to improve blood flow once

the delivery of oxygen and nutrients reaches critically low levels (i.e Critical Limb Ischemia) and

have been successful in restoring blood flow to ischemic areas[7,8]. However, not all patients

qualify for either endovascular revascularization or surgical revascularization (often elderly

patients are not good candidates and can have adverse effects), leading to a patient population that
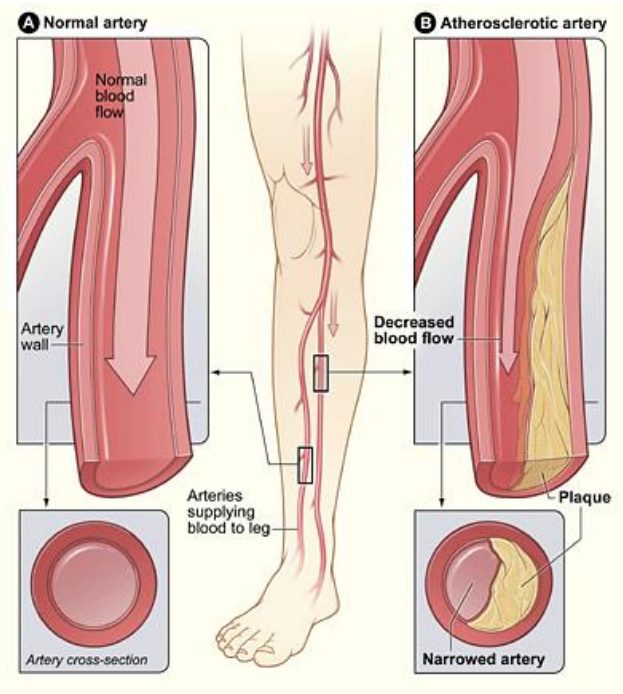
does not benefit from any approach[7,9]. There is a clear need for new therapies to improve outcomes for patients with PAOD.

One possible alternative would be to increase blood flow through the microvasculature around the affected artery, effectively forming a natural bypass. Collateral vessels (also known as arteriole anastomoses) connect arterial trees while also perfusing local muscles[10,11]. They can provide a potential bypass around an occluded artery, allowing blood from an upstream arterial tree to flow into the occluded artery downstream of the stenosis. The process by which collateral vessels enlarge by outward remodeling into larger conductance vessels is known as arteriogenesis, which provides a natural process to return blood flow to the affected tissue though the formation of a natural bypass (**Figure 2**)[11–15]. The increase in shear stress due to the rise in pressure gradient across the collateral vessel



Figure 2: Arteriogenesis returns blood flow to ischemic area. An occlusion in the main artery causes loss of blood flow and development of ischemic tissue downstream. The increase in blood flow across the collateral vessel triggers arteriogenesis and enlarges, returning blood supply to the ischemic tissue. Adapted from Chillo et al., 2016 with the permission of Cell Reports[13].

initiates the vascular remodeling process. This increased wall shear stress activates endothelial cells (ECs), which release pro-arteriogenic factors and pro-inflammatory cytokines (such as MCP-1, FGF-2, TGF-β, uPA, and MMPs), including chemokines that attract leukocytes[12,14,16–19]. Activated ECs separate and increase vascular permeability, allowing for the migration of leukocytes into the surrounding tissue[17–19]. Macrophages and monocytes adhere to ECs and later extravasate into the perivascular space where they signal other cells to begin the remodeling process[17–19]. Macrophages undergo polarization, a process by which they transition from a pro-
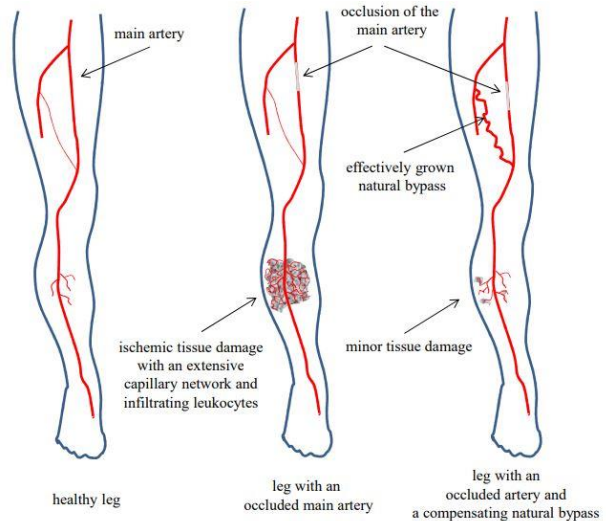
inflammatory state (M1) to an anti-inflammatory state (M2)[17,19]. The initial M1 state helps attract other leukocytes thorough the release of proinflammatory cytokines, while the M2 state releases pro-arteriogenic cytokines[19]. These pro-arteriogenic cytokines promote paracrine signaling between ECs and smooth muscle cells (SMCs) which coordinate the enlargement of the inner endothelial layer and outer smooth muscle layer through their proliferation[17–19]. The result from this cascade of events is an enlarged collateral blood vessel capable of increasing blood flow to the ischemic area. However, the extent of collateral circulation (and subsequent collateral enlargement) varies greatly among individuals due to genetic and environmental factors[20,21].

Gene and protein-based therapies have the potential to mimic arteriogenesis due to their ability to deliver growth factors to a specific area. Vascular endothelial growth factor (VEGF) is a primary regulator of arteriogenesis as it promotes endothelial cell proliferation[8,22]. Many studies have attempted to stimulate arteriogenesis by delivering recombinant human *VEGF* (rh*VEGF*) viral vectors containing the *VEGF* gene[8]. While *VEGF* delivery promotes arteriogenesis in animal models, it has had little success in human patients (only small clinical trials have been successful)[8]. Gene-based therapies experience the added issue of correctly delivering the genetic material to the target cells, which negatively impacts their success[8]. Other growth factors, including combinations of several factors, have also been studied but have had similar success to *VEGF*[8]. Arteriogenesis is a complex process that involves the expression and activity of many different proteins; this complexity combined with potentially inaccurate doses may explain the limited success of gene and protein-based therapies[8,23].

Cell-based therapies offer a new alternative to gene and protein-based therapies due to their ability to produce multiple growth factors in the correct physiological levels, mimicking the natural process observed in vivo. Candidate cell types for regenerative therapies are selected based on their regenerative role in the body. Cell therapies have also been developed around their ability to secrete growth factors and promote physiological processes. The first cell types

3

investigated to promote arteriogenesis were bone marrow-derived mononuclear cells (BM-MNCs). BM-MNCs are a combination of multiple cells found in the bone marrow, and carry out an extensive regenerative function in renovating multiple tissues such as blood vessels and neural tissues due to their multipotent capacity[24]. In response to ischemia-induced cytokines released by peripheral tissue, these cells are released into circulation and contribute to vascular remodeling. This includes the secretion of matrix metalloproteinases (such as MMP-9) which regulate the release of factors from the extracellular matrix (ECM) and secretion of further factors downstream, as well as incorporating into the vessel wall and differentiating into SMCs and ECs[24–27]. Studies using animal models found BM-MNCs enhanced arteriogenesis but these results did not translate into clinical trials[11,24]. The next cell type used was bone marrow-derived mesenchymal stem cells (BM-MSCs), originally identified in the vascular niche of peripheral tissues, which help maintain human mesenchymal tissue (connective, vascular, and lymphatic tissues)[28–30]. That these cells are routinely found adjacent to blood vessels and their role in maintaining mesenchymal tissues makes them an ideal candidate to promote vascular remodeling. Stem cells possess the ability to self-renew (formation of an identical daughter cell) and differentiate into a specific cell types, allowing for their culture and expansion, which aids in the development of the therapy[31]. Similar to BM-MNCs, BM-MSCs were successful in promoting arteriogenesis in animal models but were unable to do so in clinical patients[11]. BM-MSCs can differentiate into endothelial progenitor cells (EPCs)[28,30]. As their name suggests, EPCs, that can circulate or reside in the blood vessel wall, mature into endothelial cells that line the inside of blood vessels during vascular remodeling[28,30]. This ability has made this cell an attractive candidate for vascular regeneration therapies. EPCs are effective in animal models but have yet to demonstrate efficacy human clinical trials[24,32,33]. The progression of the different cell types for this therapy, from bone marrow derived cells to more mature EPCs, shows a trend in the pursuit of a specific cell type that regulates the vascular remodeling and the stem cell niche present around blood vessels. Myogenic precursor cells have been identified as candidates in therapies

aimed at regenerating muscle, through their transplantation and fusion with the existing tissue, but also regulate vascular remodeling[34–38]. Satellite cells (SCs) are part of the myogenic cell lineage and exist in the vascular niche where they regulate vascular remodeling, making them an ideal candidate for this therapy[34–38]. The primary function of satellite cells is to repair and regenerate myofibers, the principal component of a tissue comprising 40% of an adult human body by weight, and is composed of multinucleated syncytia surrounded by the basal lamina[39–45]. SCs reside between the sarcolemma (myofiber plasma membrane) and basal lamina in a quiescent state, mediating the regular injury-cycle due to skeletal muscle activity[39,43–50]. SCs regulate microtrauma repair by repairing/regenerating myofibers following exercise, which is one of the most effective treatments for PAOD[39,51]. SCs are also involved in enhancing microvascular growth/remodeling, and manipulating macrophage recruitment and phenotype through signaling within the local niche[39,51]. SCs are characterized by the expression of the transcription factor Pax7[39,43–50], and upon activation due to injury will begin expressing MyoD, while proliferating and maturing, with a small subset of cells undergoing self-renewal[39,43–50]. SCs undergo several rounds of proliferation before committing to the myogenic lineage, becoming myoblasts, which will mature into myocytes with the expression of myogenin[39,43–50]. At this point, myocytes will exit the cell cycle and fuse to form myotubes that can repair injured myofibers or regenerate ablated myofibers[39,43–50]. During muscle regeneration, new capillaries must grow to support the increased metabolic activity thorough angiogenesis. Angiogenesis follows a similar cascade of events as arteriogenesis with the main difference being the initial stimulus. During angiogenesis, hypoxia in the repairing tissue causes myofiber secretion of angiogenic factors; during arteriogenesis the stimulus is endothelial cell activation from the increased blood flow and subsequently increased shear stress on their surface.

The use of these cells in clinical studies for similar processes make them an attractive candidate for our proposed therapy and provide a potential fast-track to clinical testing. The effects of

presumptive SCs and their progeny on arteriogenesis have been evaluated by our group, which found that these cells enhanced collateral capillary arteriogenesis in BALB/C mice and collateral arteriogenesis C57BL/6J mice with diet induced obese (DIO), but not in lean C57Bl/6[52–54]. However, the identity of the transplanted cells was not confirmed based on transcription factor labeling, hence there is a need to verify the identity of these cells. The use of SCs for other therapies can provide valuable information on their response to transplantation to determine their constraints and advantages for this study. Specifically, clinical reports for various SC based therapies, such as treating ischemia-damaged myocardium or Facioscapulohumeral Muscular Dystrophy (FMS), can help us better understand the therapeutic potential of SCs and the logistics behind their transplantation, and therefore facilitate the development of our proposed therapy[34–38]. Use of these cells for myocardial repair depends on their ability to impact angiogenesis[15,55]. The secretion of pro-angiogenic factors by SCs enhances the angiogenic process; the similarities between angiogenesis and arteriogenesis provides a theoretical basis for the ability of SCs to promote arteriogenesis[17,35,55]. FMS studies rely on the transplantation of SCs into a specific tissue and ensuring they remain at the site of implantation, the methodology used for such studies allows us to understand the potential limitations of our cell delivery strategy[38]. The proposed approach aims to utilize the SC's ability to signal cells in the blood vessel to activate and remodel the vessel outward as opposed to muscle regeneration though SC transplantation, which would rely on their ability to fuse with existing tissue and repair damage.

To better understand the therapeutic potential of SCs for promoting arteriogenesis, we must first optimize the approach to isolate them. Myofiber isolations work by separating individual myofibers from a muscle body and culturing them to promote SC migration off the fiber onto the culture flask. Myofiber isolations can produce high purity myoblast cultures and do not require extensive purification steps such as fluorescent cell sorting (FACS) and cell preplating[56,57]. The most critical step in myofiber isolations is the enzymatical digestion of the muscle. During this

process, the excised muscle is placed in a solution containing an enzyme (e.g. collagenase II), capable of digesting connective tissue and allowing for easier separation of individual myofibers. This process involves careful regulation of enzymatical activity to ensure the muscle is sufficiently digested to yield large numbers of myofibers while avoiding over digestion and loss of myofiber viability. Other steps, such as mechanical separation of myofibers, also affect the overall yield and must be optimized along with enzymatic digestion to ensure enough SCs have been isolated for subsequent studies.

Once SCs have been isolated from whole muscle, they are expanded in tissue culture flasks to obtain a suitable amount for transplantation or in vitro characterization. Their expansion can be optimized by the addition of factors that enhance their proliferation and inhibit their differentiation. SC proliferation and differentiation is regulated by signaling from other cells found in the muscle stem cell niche[47,49]. Two major pathways identified and studied in SC culture are the basic fibroblastic growth factor (bFGF) pathway, which regulates proliferation and differentiation, and the p38 MAPK pathway, which plays a key role primarily in SC differentiation. Within the p38 MAPK pathway, a stress-activated protein kinase 2a/b (SAPK2a/b) also known as P38α/β, reversibly enhances SC quiescence by insulating the cell from external stimuli[58,59]. bFGF has been widely used in studies involving primary SC culture and has a dual role of stimulating myoblast proliferation and repressing terminal differentiation[57,60–66]. bFGF stimulates cyclin D1, a regulatory subunit of the cyclin-dependent kinases (CDK), which are expressed during the growth-1 ($G_1$) phase of the cell cycle[62–65]. Cyclin D1 regulates the transition from $G_1$ to S-phase of the cell cycle and therefore stimulates proliferation[64]. Cyclin D1 expression also inhibits myoblast differentiation[64]. Pharmacological inhibition of P38α/β promotes SC self-renewal and allows expansion of SC ex vivo with enhanced self-renewal in human SCs, while reducing terminal differentiation[67].  In both single myofiber cultures and short-term SC cultures of cell lines (MM14), SB 203580, which is a p38 mitogen-activated protein

kinase (MAPK) inhibitor that targets P38α/β, allows SCs to maintain their quiescent state. P38α/β

MAPKs are required primarily for differentiation but are also involved in proliferation[58,59,67–69].

Interestingly, satellite cells and MM14 cells supplemented with SB 203580 failed to respond to

changes in bFGF[70]. The combination of bFGF and p38 inhibition is part of our current protocol

and has demonstrated a combination of their benefits during the cell expansion phase, but their

roles are commonly regarded as being antagonistic to one another[52–54,70,71]. Initial SC isolations

did not include bFGF or SB 203580 supplementation[53]. bFGF was added to improve cell

expansion, but with the increase in cell number, SCs began to mature at a faster pace and so SB

203580 was added to reduce the rate at which these cells matured and maintain a myogenic

progenitor cell population[54,71]. From observational data, the combination of both supplements has

the potential to optimize current expansion protocols by slowing down maturation while

maintaining an actively dividing myoblast population, but we must empirically validate these

observations through studies looking at the effects of each supplement separately and combined

in varying concentrations.

High yielding SC isolations are not only required for their transplantation, it is also critical to

characterize them *in vitro*. Using fluorescent antibody labeling of transcription factors can help us

identify the phenotype of the cells in culture. As described above, Pax7 and MyoD can help us

determine if the cells in culture are myogenic progenitor cells[47]. If Pax7 and MyoD are not

present, the cell population has matured into myocytes or myotubes[47]. These strategies can be

adapted to assess cell phenotype on the transplantation vehicle. Assessment of cell distribution on

the vehicle can help us understand potential limitations in their delivery. These strategies can be

simple, such as performing live/dead staining to evaluate cell viability during different stages of

the study, to extremely complex, such as the use of superparamagnetic iron oxide nanoparticles

(SPIO) to tag transplanted cells for noninvasive visualization using MRI[72]. Regardless of the

methodology implemented, understanding both cell phenotype and distribution would allow us to assess the cellular component of the proposed therapy.

In summary, our preliminary data demonstrates that transplantation of presumptive myoblasts can promote arteriogenesis[52–54]. Confirming those preliminary results will require identification of transplanted cell phenotype, distribution, and viability, along with measurement of cell transplant efficacy in an animal model. To confirm these results, we must first obtain sufficient cells through their expansion. Cell expansion is impacted by the effectiveness of initial cell isolation and subsequent culture media optimization. Optimizing this process will require empirical determination of culture conditions which maximize in vitro expansion. Once we are able to expand our cell cultures to yield sufficient cells, we must develop a strategy for their transplantation. Transplant efficacy depends on several factors, including the vehicle used and the distribution and retention of the cells during the study. All these considerations will be summarized into the three main aims of this thesis:

- The first aim is to optimize the myofiber isolation and culture to obtain the highest number possible of satellite cell-yielding myofibers and support the initial SC culture.
    - Objective: To optimize myofiber isolation and SC culture conditions by modification of the enzymatic and mechanical digestion of the extensor digitorum longus muscle and modifying media formulation.
- The second aim is to optimize the expansion of satellite cells-derived myoblasts to promote cell expansion while minimizing differentiation.
    - Objective: To optimize culture media by modifying the dosage of bFGF and p38i supplementation to promote maximum cell proliferation and minimal cell maturation.

- The third aim will be to develop a process for evaluating the quantity and identity of isolated myogenic cells before and after transplantation and implementing all of these aims into an *in vivo* pilot study.

  o Objective: To implement an immunofluorescent transcription factor labeling protocol to determine cell phenotype.

  o Hypothesis: Myoblasts will secrete the necessary growth factors to promote arteriogenesis, leading to an increase in collateral expansion. Myocytes are too mature of a cell type to secrete the necessary growth factors for vascular remodeling and therefore not lead to an increase in collateral expansion.

# 2. METHODS

## 2.1 Animal Care

Male C57BL/6 and male BALB/c mice (Jackson Labs; Sacramento, CA) between 1 and 3 months were housed 4 to 6 mice per cage with ad libitum access to water and food (14% protein rodent maintenance diet, Envigo; Hayward, CA) in a temperature controlled facility with a 12:12 hour light:dark cycle. All procedures were completed according to protocols approved by the California Polytechnic University Institutional Animal Care and Use Committee.

## 2.2 Myofiber Isolation

Satellite cells (SCs) were obtained from single myofibers, which were isolated by enzymatic and mechanical digestion, as previously described[54]. Animals were anesthetized in an induction chamber with 5% isofluorane gas and euthanized by cervical dislocation. Animals were then disinfected with 70% isopropanol. Skin was removed from the knee to the ankle and the connective tissue around the Tibialis Anterior (TA) was blunt dissected on both hindlimbs. The distal tendon of the TA was cut, and the muscle was carefully resected to expose the underlying Extensor Digitorum Longus (EDL). The EDL was excised by cutting both distal and proximal tendons to ensure myofiber integrity. The contralateral EDL was excised closely after to avoid uneven digestion times. EDLs were immediately placed in a freshly prepared collagenase II solution (2mg·mL$^{-1}$ type 2 collagenase [Worthington LS004176] in HAMS F10 [Lonza 12-618F]) and placed in a water bath at 37ºC to digest the connective tissue/matrix. Over approximately 25 minutes, the solution was occasionally inverted, and muscles were inspected every 5 minutes. Once individual fibers appeared to start separating from muscle body, the whole muscle was transferred to a horse serum (HS, Fisher 16050122) coated 100mm petri dish (Fisher FB0875713), and filled with 20mL of wash media (20% fetal bovine serum [FBS, Fisher 10-437-028], 1% penicillin/streptomycin [Fisher SV30010] in Hams F-10 media), with a custom glass pipet coated with HS. Muscles were mechanically digested by gentle trituration using wash

media. Once enough live myofibers were isolated (~75 myofibers per T12.5 flask), they were transferred to an identical petri dish to consolidate all viable myofibers. The viable myofibers were finally transferred into a T12.5 ($12.5cm^3$) flask (Fisher FB012933) or 24-well plate previously coated overnight with ECM (Sigma E1270-1ML) and supplemented with $10ng·mL^{-1}$ bFGF (PeproTech 100-18B-100UG) and 10μM SB 203580 (p38 inhibitor, Fisher 120210) prior to incubation at 37⁰C and 5% $CO_2$. ECM is a protein solution which provides a thin coating layer promoting cell adhesion to the surface of the culture flask, it mainly consists of extracellular matrix proteins laminin and collagen IV.

## 2.3 Myoblast Culture

Once myofibers are isolated from the excised muscles, they are cultured in tissue flasks so SCs can migrate off them and can then be expanded during culture. Initial myofiber culture was left undisturbed for 3 days and imaged using an inverted microscope (Olympus CKX41). Satellite cells began to migrate off the myofibers onto the flask after one to three days in culture. On day 5, a partial media exchange was performed by transferring existing media into an equal volume of fresh growth media (wash media supplemented with $10ng·mL^{-1}$ bFGF and 10μM p38 inhibitor), lightly mixing, and transferring half of the mixture back into the flask (collecting suspended myofibers during pipetting). This approach ensures that nutrients are replenished while retaining in culture suspended myofibers that did not adhere to the flask, but are still viable and can release additional SCs onto the flask. Once local colony confluency reached ~80%, cells were rinsed with DPBS (Fisher 14-190-144) and released using a gentle dissociation buffer containing EDTA (Fisher- Gibco 13151014), leaving highly adherent cells in the flask (~1% of total cells). Released cells in media were centrifuged at 300 x g for 5 minutes, the supernatant aspirated, and precipitated cell pellet resuspended in warm, fresh growth media and counted using a manual hemocytometer counter (INCYTO DHC-N01-5). To continue expansion, cells were seeded on a T25 flask ($25cm^3$, Fisher 10-126-10), which was coated overnight in ECM. To immunostain, cells

were plated for 12 hours and fixed on 8-well chamber slides (Fisher 12-565-8). Alternatively, cells were also resuspended after centrifugation in 80% FBS (Fisher SH3091003) and 20% DMSO (SIGMA D2650) for cryopreservation. To determine optimal supplement dosage, individual fibers were cultured separately in a 24-well plate (Fisher 3526) for 3 days. For the in vivo study, separate myoblast and myocyte populations were prepared to ensure the appropriate cell type was transplanted for each group. The myocyte group was prepared using the same culture techniques previously described but removing the p38i from the culture media during complete culture to promote cell maturation.

## 2.4 Immunofluorescence

Cell phenotype was explored based on myogenic transcription factor expression using immunofluorescent labeling. Cells were fixed in 4% paraformaldehyde (PFA, Fisher 50-980-487) at room temperature for 10 minutes, rinsed with DPBS, and then permeabilized in 0.5% Triton X-100 (VWR M236-10ML-5PK) in DPBS for 5 minutes. Blocking solution (UltraCruz Blocking reagent, Santa Cruz Biotech sc-516214) was added for 30 minutes before incubating fluorescently labeled primary antibodies in blocking solution (1:200, Pax7 and MyoD from Novus Bio NBP2-34706AF594 and NB10056511F, respectively) for 60 minutes at room temperature. Primary antibodies were conjugated with Alexa 594 and FITC, respectively. Coverslips were sealed with DAPI-containing mounting medium (Santa Cruz Biotech sc-359850) prior to image capture with an Olympus BX41 widefield fluorescent microscope and QCapture pro. Images were captured at 10X and 20X magnification and analyzed using Image/J.

## 2.5 Gelatin Hydrogel Preparation

To deliver the cells to the target area, a gelatin hydrogel vehicle was prepared. After boiling to dissolve, a 10% (w/v) gelatin (Sigma G1890-100G) solution was dispensed into wells of a 24 well plate and left to polymerize for 30 minutes. The polymerized hydrogel was then incubated in sterile 6mM 1-ethyl-3-(3-dimethylaminopropyl)carbodiimide hydrochloride (EDC, Fisher

PIPG82079) to crosslink the gelatin overnight at 4ºC. Gelatin was washed with sterile $H_2O$ 3x for 30 minutes prior to cell seeding at a density of $2.5x10^5$ cells·cm$^{-2}$; seeded gelatin was incubated at 37ºC for 12 hours.

## 2.6 Femoral Artery Ligation and Transplantation

Animals were initially anesthetized in an induction chamber with 5% isofluorane in oxygen. Once anesthetized, isofluorane was maintained at 1-3% and a flow rate of 0.5-1.5 min$^{-1}$. Animals were weighed and provided analgesic (buprenorphine at 0.075 mg/kg). The surgical area was depilated and then disinfected with chlorohexidine diacetate (Nolvasan). Animal internal temperature was maintained by a heat pad placed under the surgical stage controlled by a rectal thermistor. Ophthalmic ointment was applied to prevent corneal desiccation. An initial incision was made parallel to the femoral artery directly near the epigastric fat pad, and connective tissue was blunt dissected. Once the neurovascular bundle was exposed, the femoral artery was carefully isolated. Using 7-0 silk suture, the femoral artery was ligated distal to the epigastric and proximal to the popliteal arteries. Gelatin hydrogels were prepared using a 2mm biopsy punch and placed in a 'pocket' that was prepared by undermining the gracilis muscles. The incision was then closed using 7-0 prolene suture. Post-operative analgesia was delivered every 24 hours for 3 days. The same procedure was performed on the contralateral hindlimb with the exception of artery separation, femoral artery ligation, and gelatin hydrogel transplantation. This procedure was performed with the assistance of Ada Tadeo and Jaden Frazier.

## 2.7 Functional Vasodilation

To assess the effects of myoblast transplantation on arteriogenesis, functional vasodilation was performed to explore changes in collateral outer diameter and function. The construct was also retrieved to explore the effects of transplantation on the cells. Seven days post transplantation, animals were anesthetized and prepared as described above. A skin incision was made directly above the anterior gracilis to expose it, and the gelatin hydrogel was removed and placed in PBS

14

for evaluation. To stimulate muscle contraction, tungsten microelectrodes (FHC- PBSA1075) were placed on the surface of the gracilis, midway between the saphenous and profunda arteries; an intravital microscope (Olympus BXFM) was positioned above the collateral midzone and the exposed area was covered with plastic wrap. After a 30-minute equilibration period, the muscle was stimulated for 90 seconds at 8Hz with 1mA stimuli of 200μs duration; images were captured immediately following the cessation of muscle contraction. Sodium nitroprusside ($1x10^{-4}$) and norepinephrine ($1x10^{-4}$) were dripped over the muscle to maximally dilate and constrict the collateral vessel, respectively. This procedure was repeated for the contralateral hindlimb. This procedure was performed by Ada Tadeo.

## 2.8 Vascular Casting

To explore changes in collateral inner diameter and vessel wall thickness, vascular casting was performed. After the functional vasodilation assessment, animals were prepared for vascular casting using Microfil [Flow Tech Inc. MV-120]. Through a left ventricular cannula, vasodilator cocktail (400 μL Heparin, 25 mM Sodium Nitroprusside, and 1.5 mM Adenosine in 38mL of PBS) was perfused at a rate of 5 mL·min$^{-1}$ to clear the circulation of blood and fixation solution (4% paraformaldehyde in PBS) was perfused at a rate of 4 mL/min to preserve the tissue. Once the femoral artery had been cleared of blood and fixed, the Microfil was perfused via the same left ventricular cannula at 0.5 mL·min$^{-1}$. Once the vascular cast was complete, the animal carcass was stored at 4°C overnight. The gracilis muscle was then excised and placed in a microcentrifuge tube containing 2% Triton X-100 in PBS for 2 hours at room temperature to permeabilize the muscle. The muscle was then incubated in a 1:400 Anti-Alpha Smooth Muscle Actin antibody [Sigma Aldrich C6198] solution in a 2% Bovine Serum Albumin (BSA) [Sigma Aldrich A2153] and PBS solution for 96 hours at 4°C in the dark. The muscle was washed with 0.1% Triton X-100 in PBS 3x for 10 minutes and then in PBS for 30 minutes prior to slide

mounting in a solution of 50:50 PBS:Glycerol [Sigma Aldrich G7757]. This procedure was performed by Jaden Frazier.

2.9 Image Analysis

Vessel diameters and cell counts were performed with ImageJ software using the line measuring tool and multipoint tool, respectively. Vessel diameter was measured 5 times to determine average diameter and 3 independent cell counts were performed for each sample to determine average cell count.

2.10 Statistical Analysis

Statistical analysis was performed using Minitab statistical software. Differences in cell counts and transcription factor expression for changes in media supplementation, as well as differences in resting and dilated vessel diameters and collateral wall thickness between treatment groups were determined using one-way ANOVA and compared via Tukey post-hoc comparisons. A p-value of less than 0.05 indicated statistical significance. Values are presented as mean values with standard error (mean $\pm$ SE).

# 3. RESULTS

Developing a myogenic cell therapy to enhance arteriogenesis, aimed at patients suffering from PAOD, requires a robust methodology which allows us to assess the different components separately and then combined during a pilot study. From our preliminary data, we found that presumptive myoblasts can enhance arteriogenesis[52–54]. Hence, our goal is to replicate that study after including a more extensive assessment of the cell therapy candidate to overcome the limitations from previous studies, including the lack of cell characterization both during culture and after transplantation. This refined methodology includes an optimization of the initial isolation and culture of the target cell type, their characterization based on specific transcription factors during different stages of their culture, as well as on the transplantation vehicle pre- and post-transplantation, culminating in a final pilot study combining all previous studies with an evaluation of the impact of myogenic cell transplantation on arteriogenesis.

Satellite Cell Morphology

To determine the different morphological stages of myogenic cells under the culture conditions used in this study, images of the cultures were captured at different stages and stained for Pax7 and MyoD transcription factors to confirm their phenotype (**Figure 3**). Four main stages of SC morphology were observed during culture. Initially, presumptive SCs on the surface of myofibers appeared round upon transfer of myofibers onto culture dish (**Figure 3A**). As they migrated off the myofiber and adhered to the surface of the culture flask they began to elongate and adopt a triangular shape from day 1 to day 8 (**Figure 3A, B**). Myogenic cells that remained in culture for extended periods of time (more than 10 days) and formed confluent presumptive myocyte populations (~80%) that appeared to commit to a final maturation by elongating and orienting themselves in arcing patterns (**Figure 3C**). These presumptive myocyte populations would then to fuse and form large multinucleated myotubes (**Figure 3D**), which were initially (around 20 days after isolation) surrounded by myocytes and did not exhibit spontaneous contraction. As the

remaining myocyte population fused together, myotubes began to mature and were capable of

spontaneous contraction (**Figure 3E**). Samples from early cultures in which SCs had recently

migrated off myofibers were positive for Pax7 and MyoD, confirming their identity as early

myogenic progenitors (**Figure 3F, G, H, I**). Samples of cultures at stages in which cells began to

elongate and orient themselves stained negative for Pax7 and MyoD, confirming they were no

longer myogenic progenitor cells (**Figure 3J, K, L**). Using these results and the distinct

morphological changes observed during myogenic cell culture, we were able to estimate

phenotype based on a morphological assessment of the cells. These estimations allowed us to

quickly evaluate myogenic cultures by visual observation during the culture and expansion stages

of cells for transplantation. Now that we were able to determine the identity of the cells in culture,

we began optimizing their isolation.
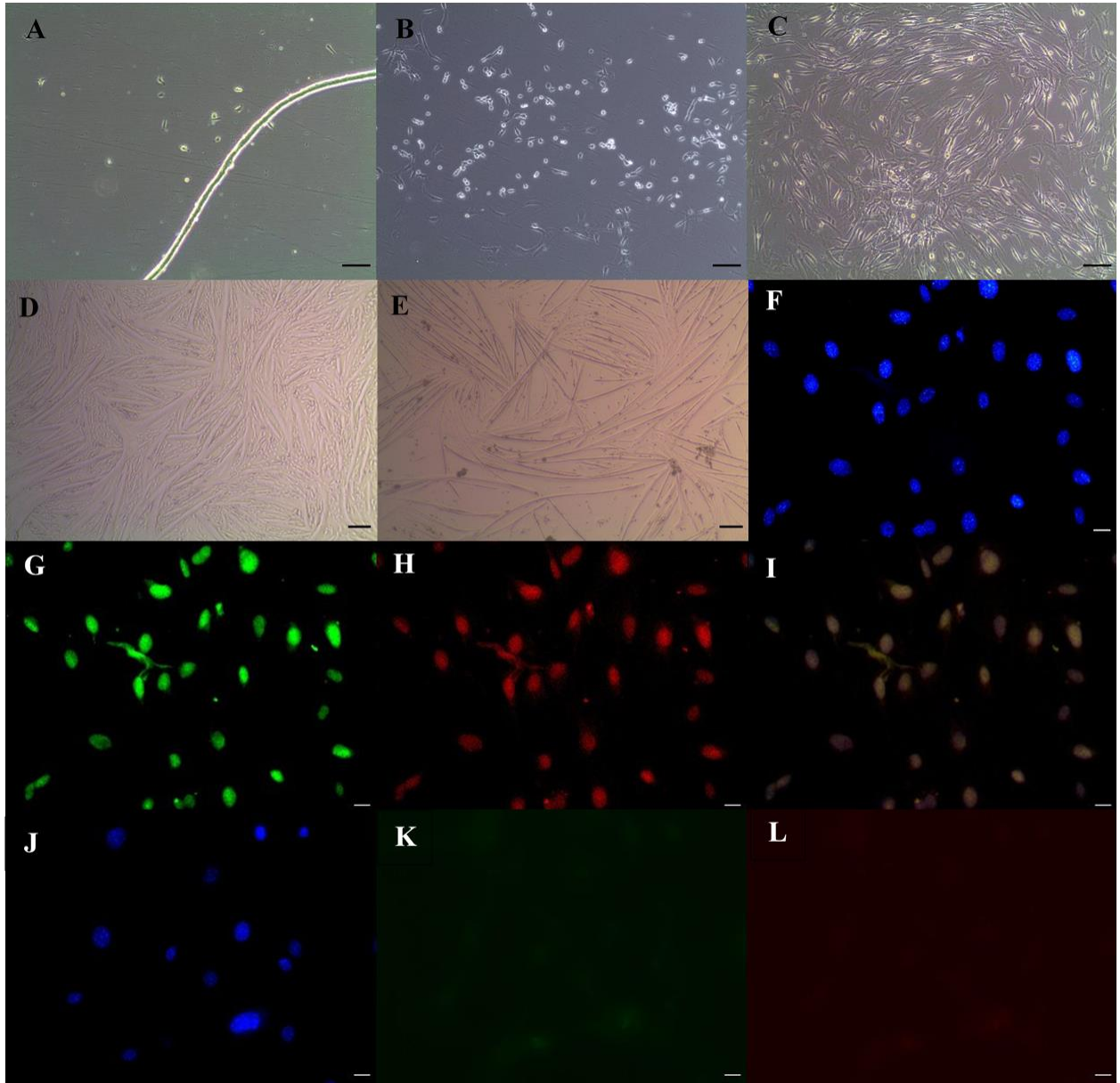
Figure 3: Progression of primary isolated myogenic cells during in vitro culture. A, presumptive satellite cells recently migrated from a myofiber (Scale bar 100µm). B, presumptive myoblasts expanding during culture (Scale bar 100µm). C, presumptive myocytes beginning to align in dense formations (Scale bar 100µm). D, Early multinucleate myotubes surrounded by myocytes (Scale bar 200µm). E, Mature myotubes capable of spontaneous contraction (Scale bar 20µm). F, G, H, I, Immunofluorescent labeling of MyoD (G) and Pax7 (H) in 100% of nuclei (F) confirmed myoblast phenotype in population/similar population as (B), MyoD, Pax7, and DAPI merged image (I) (Scale bar 20µm). J, K, L, Absence of immunofluorescent labeling of MyoD (K) and Pax7 (L) in 100% of nuclei (J) confirmed myocyte phenotype in population/similar population as (C) (Scale bar 20µm).

Myofiber Isolation Optimization

To perform multiple studies on the behavior of SCs in vitro and perform a pilot study to
determine their impact on arteriogenesis, a robust method to maximize cell yield was required to
obtain sufficient cells. To develop more efficient cell isolation procedures, a number of isolations
were performed under different conditions and evaluated using cell number at various stages in
the culture. **Figure 4** displays cell number from each passage of 6 select isolations in
chronological order (**Figure S1** in **Appendix C** contains additional images of the myofiber
isolation process). *Table 1* summarizes the changes made between isolations and the results
observed after they were implemented. We can broadly group these changes into 3 categories:
mechanical and enzymatical digestion methods, and media supplementation. Initial changes in
enzymatical digestion methods included changing from frozen to freshly prepared collagenase II
solutions. The effects from this change were immediately observed, as the time required for
enzymatical digestion decreased from ~45 minutes to ~20 minutes, but the more critical effect
was the improved separation of myofibers from the entirety of the muscle body, even deep inside
the muscle. While frozen collagenase II solution would release myofibers on the surface of the
muscle, the fresh solution separated fibers deeper inside the muscle and allowed for faster and
higher yielding myofiber isolations (*Table 1*, Isolation 3). Mechanical digestion improvements
came from improving the connection between the micropipette and the custom glass tip to ensure
an airtight seal. This allowed for greater control over media flushing and myofiber collection,
leading to a greater number of myofibers isolated and reducing shear stress during transfer, which
could result in myofiber death (*Table 1*, Isolation 2). After changing bFGF and p38i dosages, SC
migration from myofibers and expansion of myogenic cells in culture improved. Increasing
supplements of bFGF increased SC number, while greater inhibition of p38 MAPK reduced
myogenic cell maturation. Finally, improvements in technique included smoother and more
controlled flushing of media, which may have reduced the stress on the myofibers and increased

the amount of viable myofibers isolated, as well as transferring only viable myofibers into the final petri dishes to avoid introducing dead myofibers into the culture flask. These improvements were a result of performing multiple isolations, implementing these techniques, and observing how they affected myofiber isolation and viability. All the changes during this objective lead to the initial optimization of isolating myofibers from muscle increasing day-10 yield by nearly an order of magnitude, from $3 \times 10^5$ to $1 \times 10^6$ cells. Having made most gross changes to the isolation protocol, the next step was to empirically optimize the effect of media supplementation on initial SC migration from myofibers.

Table 1: Myofiber Isolation Optimization Results Summary

| Isolation | Changes (based on previous isolation) | Result |
|---|---|---|
| 1 | bFGF Dose: 2 ng/mL  p38i Dose: 5 µM  Frozen Collagenase II solution | Cell counts: $3 \times 10^5$ (Day 10) |
| 2 | Improved pipette connector | Higher number of myofibers isolated (+50%)  Cell counts: $7 \times 10^5$ (Day 10) |
| 3 | Fresh Collagenase II solution | Higher number of myofibers isolated (+100%)  Cell counts: $3 \times 10^5$ (Day 8), $4 \times 10^5$ (Day 10), $6 \times 10^5$ (Day 18) |
| 4 | bFGF Dose: 10 ng/mL | Myoblasts began to mature into myocytes  Cell counts: $7 \times 10^5$ (Day 7), $1.2 \times 10^6$ (Day 10), $4.25 \times 10^6$ (Day 17) |
| 5 | p38i Dose:10 µM | Lower myoblast maturation  Cell counts: $6 \times 10^5$ (Day 7), $9 \times 10^5$ (Day 9), $1 \times 10^6$ (Day 12) |
| 6 | Refined myofiber isolation technique | Cell counts: $4 \times 10^5$ (Day 3), $1.1 \times 10^6$ (Day 7) |
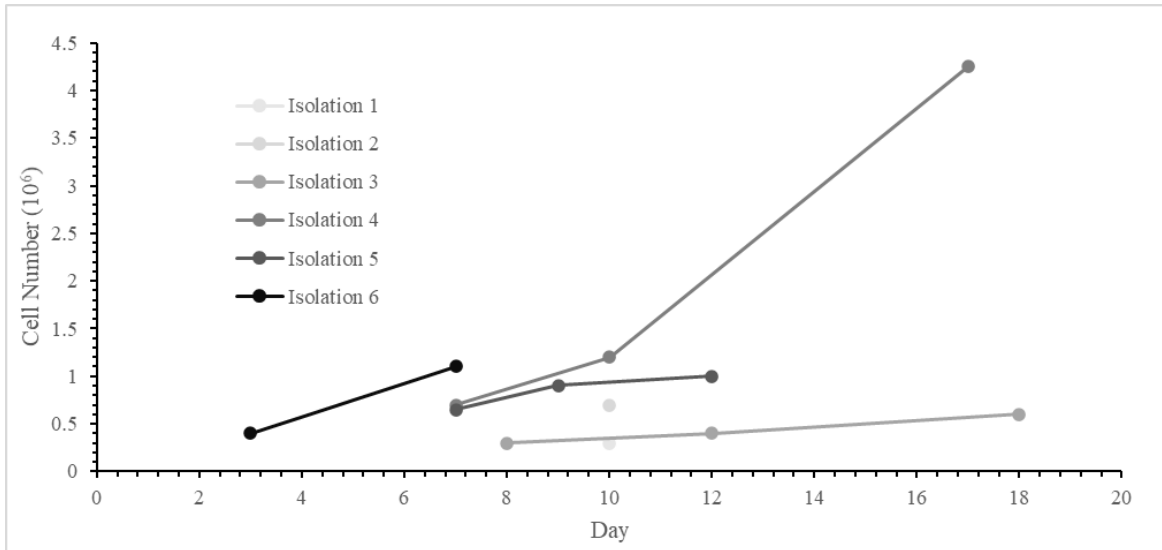
Figure 4: Cell number counts for select isolations. Evolution of cell number evaluated upon passage during isolation protocol optimization starting from isolation 1 to isolation 6.

Supplement dosage response for initial myogenic cell migration and early expansion

Once we were able to efficiently isolate myofibers from muscle, we optimized bFGF and p38i supplementation to ensure optimal migration and initial expansion of SCs from myofibers. To maximize SC migration and initial expansion, media formulation was optimized by modifying bFGF and p38i concentration. We explored the impact of varying concentrations of bFGF and p38i on individual myofibers by applying different concentrations of bFGF and p38i in separate wells of a 24 well plate (**Figure 5**). P38 inhibitor dose was varied (0X, 0.5X, 1X or 10μM, 2X) while keeping bFGF dosage constant (1X or 10ng/mL) and vice versa; a control culture containing no p38 inhibitor and no bFGF was also included). Myogenic cells that migrated off the fibers were counted on days 1 and 3, and the fold increase for each treatment group was calculated to compare the increase in cell number with the supplement concentration. bFGF increased the number of cells migrating and expanding in the first 3 days of culture in a dose-dependent manner (**Figure 5C**). SC count increased until the 1X dose (5.97 ± 0.50), at which point the effect of bFGF supplementation plateaued, as no further increase was detected when its concentration was doubled (6.83 ± 0.65). Supplementation using the 0.5X dose (4.17 ± 0.35) had

no effect on cell counts when compared to the 0X and No supplementation groups ($3.36 \pm 0.36$ and $3.56 \pm 0.29$ respectively). Inhibiting p38 MAPK had no impact on cell number (**Figure 5D**) at the 0.5X and 1X doses, ($5.40 \pm 0.31$, and $5.97 \pm 0.50$ respectively), but reduced proliferation at the 2X dose ($3.56 \pm 0.29$). Surprisingly, the 2X dose lowered proliferation to the level of the no supplement groups. The highest p38i dose that would not impact cell expansion and would reduce myoblast maturation was determined to be the 1X dose. Optimal supplement concentration, with regards to cell expansion, was 1X bFGF and 1X p38i. These supplement concentrations were implemented to optimize cell expansion and maintain cell phenotype during migration from myofibers and initial culture.
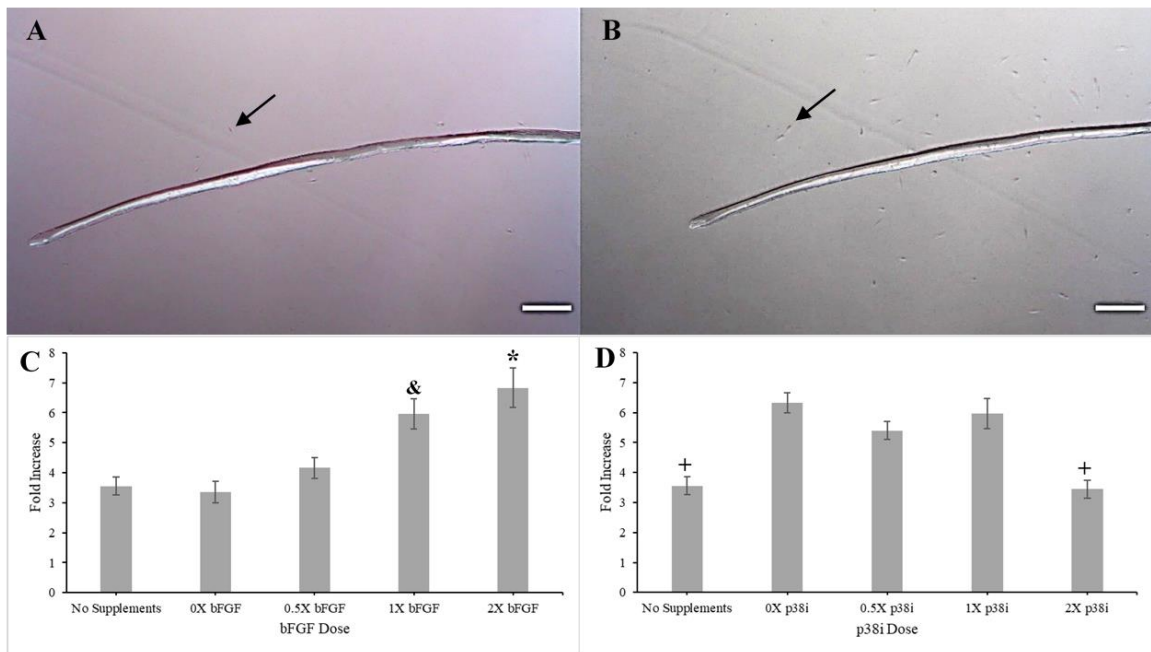


Figure 5: Initial myogenic cell migration and expansion in response to changes in bFGF and p38 inhibitor supplementation. A, Satellite cell migration after 1 day in culture (Black arrow: Satellite cell, scale bar 200µm). B, Satellite cell migration after 3 days in culture (Black arrow: Satellite cell, scale bar 200µm). C, Fold increase in myogenic cell number between culture day 1 and 3 in response to changes in bFGF supplementation (*, $p<0.05$ vs 0.5X, 0X, and No supplements, &, $p<0.05$ vs, 0X, and No supplements). D, Fold increase in satellite cell number between culture day 1 and 3 in response to changes in p38 inhibitor supplementation (+, $p<0.05$ vs 1X, 0.5X, and 0X). n=3 wells for each supplement combination)

Effects of supplements on SC expansion and differentiation

Myoblasts kept in culture for extended periods of time (past 72 hours) begin to mature at a faster rate and start to lose proliferative ability. To maximize cell expansion and minimize maturation of myoblasts, cultures were supplemented with bFGF and p38i, either factor, or neither factor. Myogenic cells were cultured for 7 days, before assessing morphology, cell number, and phenotype (**Figure 6**). Cultures were passaged before reaching more than 80% local confluency to avoid effects of increased cell density on phenotype, as overly confluent cultures were observed to promote myoblast maturation. Only the culture supplemented with both p38i and bFGF reached confluency and was passaged on day 5. bFGF increased cell number compared to the no-supplement control ($8.6 \pm 0.03$ [x$10^5$] vs $0.43 \pm 0.02$ [x$10^5$]). The p38 inhibitor did not increase cell number ($0.53 \pm 0.02$ [x$10^6$]), but also did not affect bFGF-enhanced proliferation ($0.96 \pm 0.04$ [x$10^6$]) (**Figure 6E**). The impact of bFGF and p38i on differentiation was assessed by phenotyping the cultures using MyoD and Pax7 as markers of early myogenic progenitor cells. bFGF had no effect on MyoD expression, bFGF alone did not increase MyoD expression ($92.9 \pm 4.3\%$) when compared to other treatments (no supplements $81.1 \pm 4.5\%$; p38i only $99.2 \pm 0.8\%$), but also did not affect the enhancement of MyoD expression by p38i ($100 \pm 0\%$, **Figure 6F**). P38i alone however, increased MyoD expression as compared to the non-supplemented group. There was no difference between p38i supplemented groups and bFGF only supplemented groups (**Figure 6F**). Pax7 expression was not affected by bFGF or p38i but follows similar trends as MyoD expression (**Figure 6G**). This evaluation of the effect of the bFGF and p38i supplementation on 7-day expansion and phenotype suggest that bFGF supplementation supports myoblast expansion but not MyoD and Pax7 expression. Conversely, p38i supplementation does not increase myoblast expansion but does increase MyoD expression and seemed to have a positive trend with respect to Pax7 expression. Maintaining MyoD and Pax7 expression is desirable to maintain an early myogenic cell population which is highly proliferative. Due to the

high adherence of mature cell types (mentioned in the myoblast culture methods), the results shown in **Figure 6** represent the maximum percentages of Pax7 and MyoD expression since mature cell types which do not express either factor remained in the culture flask during passaging. This results in smaller differences between treatment groups and does not fully reflect the effects of the p38i supplementation. The actual differences between groups are likely to be larger than the one illustrated below. The combination of both supplements seems to have the highest potential as the optimal media formulation for cell expansion post migration and maintaining the population at an early myogenic cell phenotype.
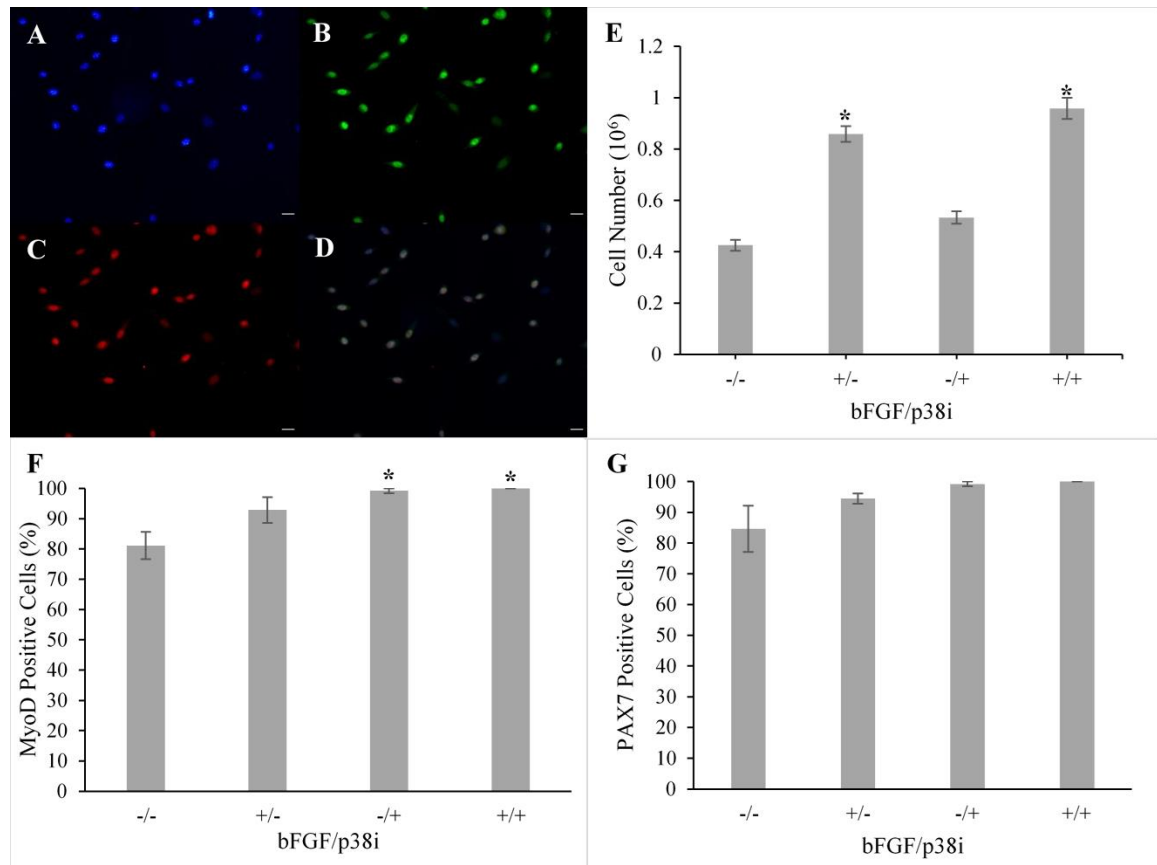


Figure 6: Effects of bFGF and P38 inhibitor supplementation on 7-day satellite cell culture. A, B, C, D, Immunofluorescent labeling of MyoD (B) and Pax7 (C) in nuclei (A) at day-7 following myofiber isolation; merged image (D) (Scale bar 20µm). E, Effects of bFGF and P38 inhibitor supplementation on day 7 myoblast cell number (*, $p<0.05$ vs -/- and -/+), MyoD expression (F) (*, $p<0.05$ vs -/-), and Pax7 expression (G) in day 7 myoblasts. One separate isolation per treatment was performed and repeated 3 times (n=3).

Evaluation of the gelatin hydrogel vehicle

After optimizing the isolation and culture of SCs and developing a methodology to characterize them, we prepared them for transplantation. For this process we adapted our characterization methodology to visualize cell phenotype on gelatin and determine cell viability. To assess the viability of the gelatin hydrogel vehicle for cell delivery, cell viability and cell phenotype were evaluated pre- and post-transplantation (**Figure 7**). Cells were plated on the gelatin hydrogel construct 12 hours pre-transplantation. To determine cell viability on the hydrogel and ensure live cells were transplanted, a live/dead stain was performed prior to transplanting. Cell viability was close to 99% (n=3) at 12 hours after plating for both myoblast and myocyte groups, with most of the dead cells suspended in media instead of adhered to the hydrogel (**Figure 7A**). After the 7-day transplantation study, the constructs were retrieved from the implant site for evaluation of viability and myoblast phenotype. Cell viability 7 days post transplantation was <1% (n=3) for the myoblast and myocyte groups (**Figure 7C, D**). No groups expressed MyoD or Pax7 (**Figure 7J, K, L**). Interestingly, the gelatin vehicle contained live and dead cells adhered on the construct (**Figure 7E, F**). Implementation of the live/dead stain and adaptation of the characterization methods were initially hindered by the inability to perform the necessary washing step during immunofluorescent staining due to the construct's physical properties, which made quantification challenging. This was resolved by modifying the image acquisition parameters to filter out low fluorescent signals. After evaluation of cell phenotype on the gelatin hydrogel pre- and post-transplantation, we determined that this vehicle allows us to transplant live cells after a 12-hour plating period. From the post-transplantation results, we can observe that cell viability at day 7 is absent and MyoD and Pax7 expression is also low.
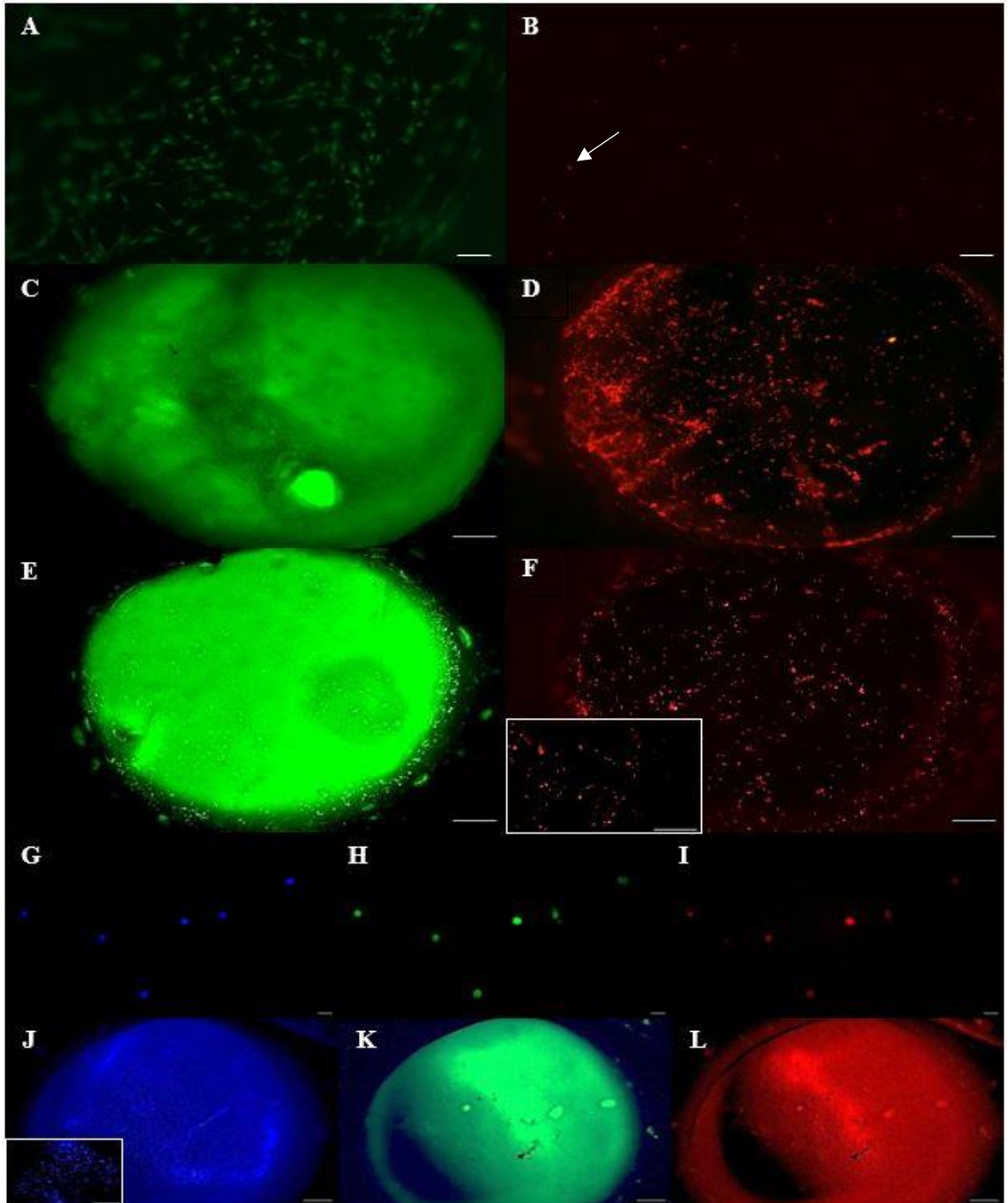
Figure 7: Evaluation of myoblasts on gelatin hydrogel. Live (A) dead (B) (white arrow) myoblasts on gelatin 12 hours post-plating (Scale bar 100µm). Live (C) dead (D) myoblast-construct on gelatin 7 days post-transplantation (Scale bar 200µm). Live (E) dead (F) cells of gelatin vehicle 7 days post-transplantation (Scale bar 200µm, magnified image of dead stain on bottom left corner, scale bar 100µm). Immunofluorescent labeling of MyoD (H) and Pax7 (I) in myoblast nuclei (G) 12 hours post-plating on gelatin (Scale bar 20µm). Immunofluorescent labeling of MyoD (K) and Pax7 (L) in nuclei (J) of myoblast-constructs 7 days post-transplantation (Scale bar 20µm) (Magnified image of DAPI stain on bottom left corner, scale bar 100µm).

In vivo evaluation of myoblasts and myocytes on collateral function and structure

To determine if myoblast or myocyte transplantation enhances collateral size and maturity, cells were plated and transplanted (**Figure 8**) deep to the gracilis muscle during femoral artery ligation in BALB/C mice. At 7-days following surgery, gracilis collaterals were imaged using intravital microscopy to measure collateral diameter (**Figure 9A, B**). Myoblast and myocyte groups had no effect on maximum collateral diameter when compared to the vehicle only group (**Figure 9C**). From these results, we cannot conclude that myogenic cell transplantation enhanced collateral expansion. Other possible effects, such as acceleration of collateral maturation could have occurred. This was determined by assessing vascular tone and resting diameter, which was not impact by the cell transplantation. These were measurements of internal diameter and did not take into account the collateral wall thickness; myogenic cell transplantation may have increased vascular smooth muscle proliferation and therefore collateral wall thickness. Therefore, collateral wall thickness was assessed by subtracting the luminal diameter, determined from a vascular cast, from the outer diameter, determined by an α-smooth muscle actin stain (**Figure 10A, B**). No difference in collateral wall thickness was found between treatment groups (**Figure 10C**). These results suggest that myoblast or myocyte transplantation did not promote collateral enlargement, vascular wall growth, or maturation.
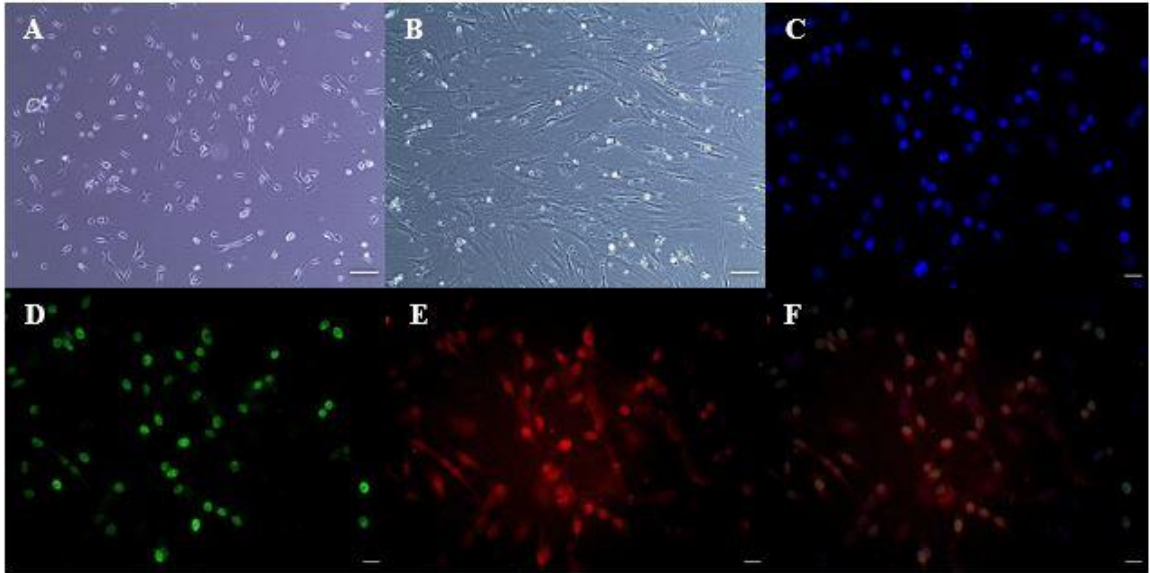
Figure 8: Myogenic cells transplanted for in vivo evaluation. A, Myoblasts isolated from BALB/c donor mouse pre-transplantation (Scale bar 100µm). B, Myocytes isolated from BALB/c donor mouse pre-transplantation (Scale bar 100µm). C, D, E, F, Immunofluorescent labeling of MyoD (D) and Pax7 (E) on myoblasts pre-transplantation compared to a DAPI nuclear stain (C) and merged (F) in a single image (Scale bar 20µm).
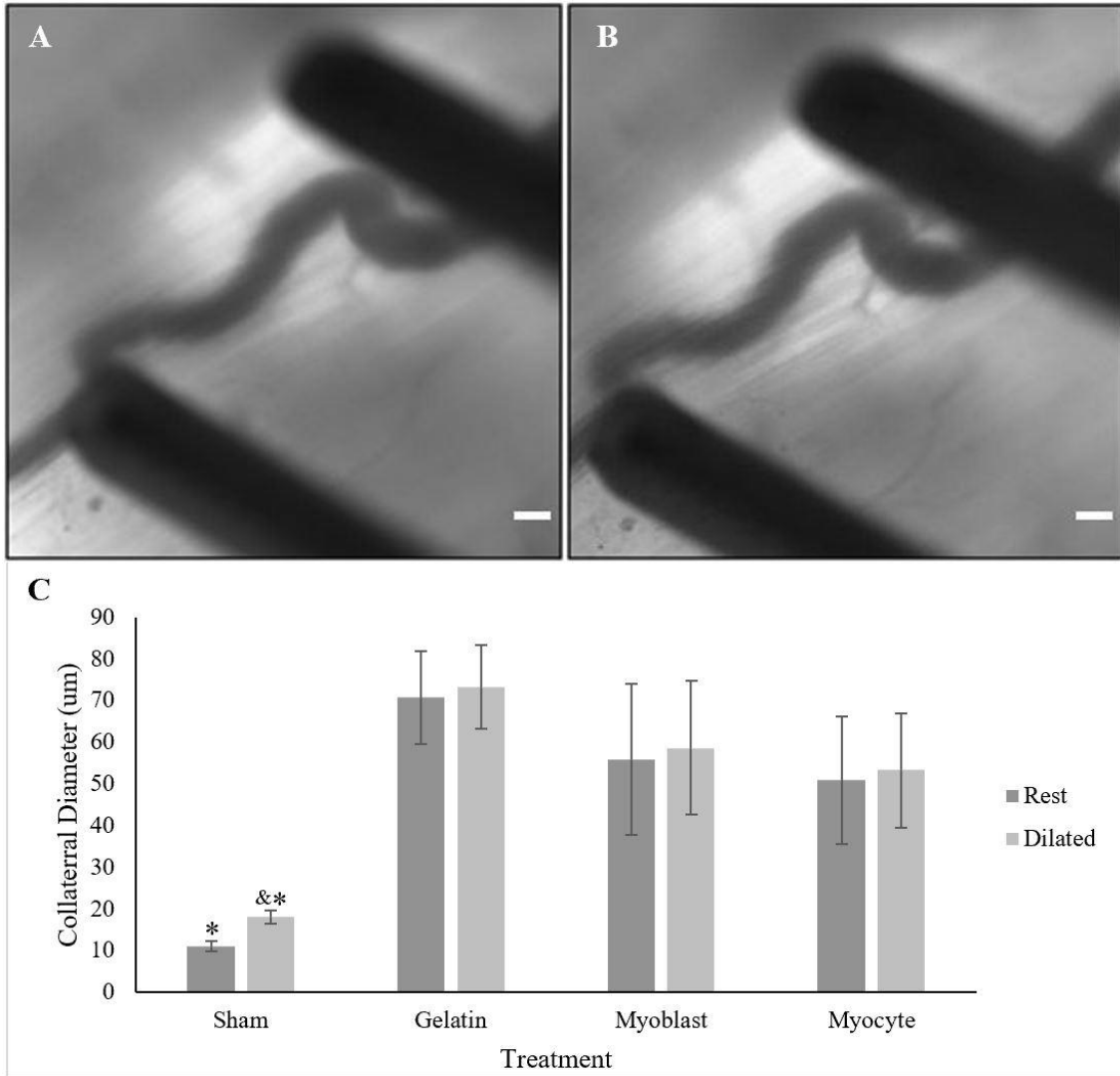
Figure 9: Collateral mean diameter measurements before and after electrical stimulation.
Intravital collateral image after myoblast transplantation before (A) and after (B) electrical
stimulation (Scale bar 50µm). C, Functional vasodilation and collateral diameter comparison
between treatment groups (Myoblast group n=3, Myocyte and gelatin groups n=4, Sham group
n=11, *, $p<0.05$ vs Gelatin, Myoblast, Myocyte, &, $p<0.05$ vs Sham Rest). Data collected and
analyzed by Ada Tadeo.
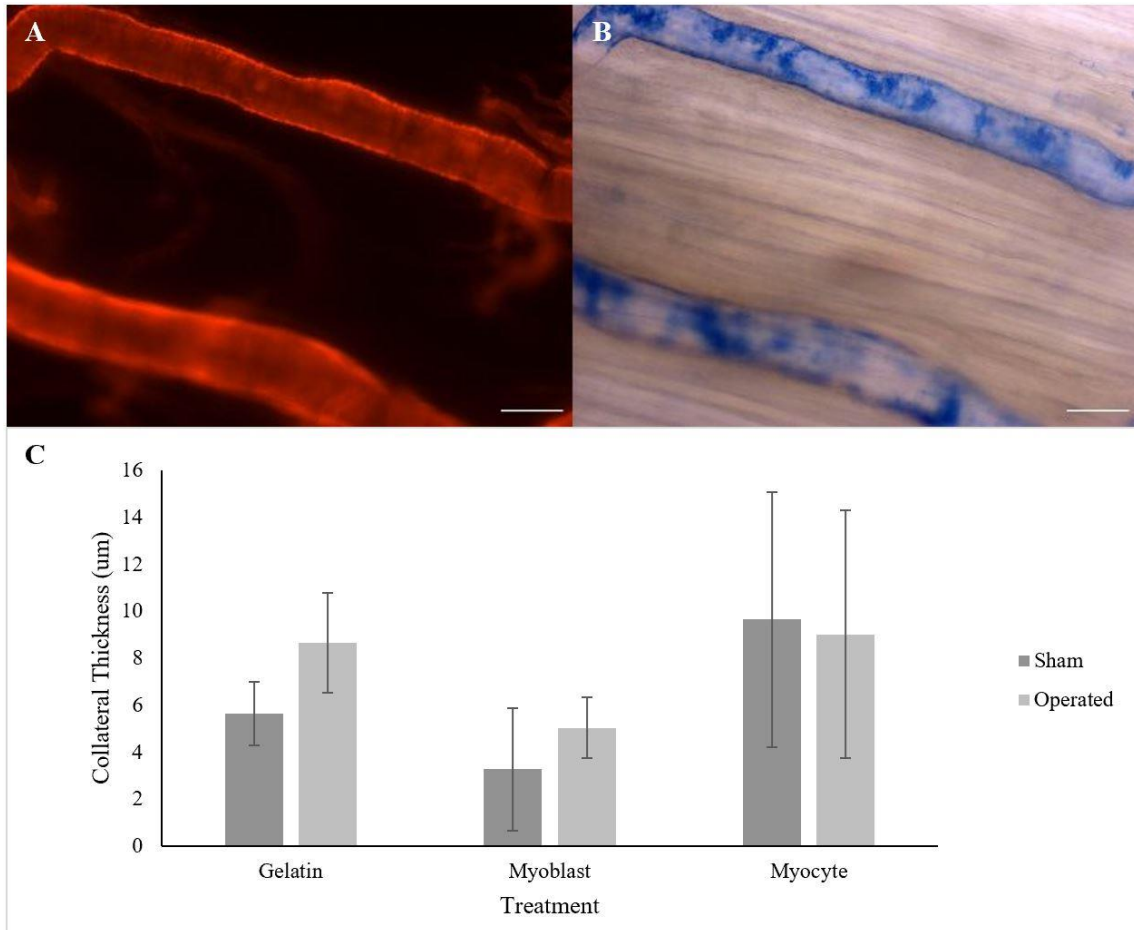
Figure 10: Collateral vessel wall mean thickness measurements. A, Collateral vessel outer diameter stained using α-smooth muscle actin after myoblast transplantation (Scale bar 100µm). B, Collateral vessel filled with microfil after myoblast transplantation (Scale bar 100µm). C, Collateral wall thickness compared between treatment groups for sham and operated hindlimbs (No significant differences observed). Data collected and analyzed by Jaden Frazier.

# 4. DISCUSSION

Peripheral arterial occlusive disease (PAOD) is characterized by the development of atherosclerotic plaques in the larger peripheral arteries, which decreases blood perfusion to peripheral tissues and causes ischemia[1]. With the limited selection of potential treatments and their reported low efficacy, cell therapies have been proposed as alternate therapy candidate to promote collateral arteriogenesis and provide a natural bypass to return blood perfusion to the affected tissues[7,9]. Myogenic progenitor cells play an important role in muscle regeneration and secrete a wide range of growth factors involved in macrophage recruitment and arteriogenesis[41,43]. The potential of altering the local niche to promote collateral arteriogenesis makes these cells an attractive candidate for treating PAOD. Early preliminary studies evaluating the impact of presumptive myoblast transplantation on arteriogenesis found that these cells can enhance arteriogenesis[52–54]. However, after failure to enhance arteriogenesis in later preliminary studies, the focus of this study was to address the limitations related to myoblast isolation and characterization. The first aim of the study was to update the myoblast isolation and culture methodology and develop a reliable and effective approach to obtain sufficient cells of the required phenotype to perform further studies. The second aim this study addressed was confirming the identity of the cells transplanted using specific transcription factors, as well as characterizing and assessing the viability of cells on the vehicle before and after transplantation. A pilot study, similar to previous preliminary studies, was performed to synthesize all the aims of the study and implement these newly developed methods to determine the effect of myoblast transplantation on collateral arteriogenesis, while evaluating the cellular component of the therapy during the study.

Initial Cell Phenotype and Morphology Assessment

Previous approaches to characterize myogenic cells by our group involved morphological assessment of isolated cells to determine their phenotype[71]. To reliably use such a strategy, we

32

must first confirm the identity of cell type using more robust methods to correlate/extrapolate the morphology of these cells at different stages in the myogenic lineage. The first step of this characterization process was to confirm that the isolated cells were indeed satellite cells (SCs) and their progeny. To confirm this, we kept the isolated cells in culture and grew them until they matured into myotubes, confirming their myogenic identity. Having confirmed the myogenic potential and apparent absence of contaminating cell types, we assessed SC morphology during all stages of myogenic cell culture and confirmed these observations with transcription factor identification. Confirming the phenotype using transcription factor labeling and comparing these to the morphology of the cells allows us to quickly infer myogenic cell phenotype based on visual observation. This allows the individual culturing these cells to quickly assess the myogenic state of the culture by inspecting the culture flask during passaging or feeding procedures. It was determined that myogenic cells displayed four distinct stages during culture. They initially presented as small round perturbations on the surface of myofibers and remained like this upon initial migration onto the surface of the culture flask, at which point they would elongate and appear triangular in shape. Myogenic cells would then initiate their commitment to terminal differentiation and maturation, starting to elongate and orient themselves before finally fusing together and forming myotubes. These stages were confirmed by the expression of Pax7 and MyoD transcription factors during the earlier stages of culture, when cells were immature myoblasts, and the absence of these transcription factors in later stages, when cells elongated and became myocytes and myotubes. Pax7 and MyoD are expressed by early myogenic progenitor cells, i.e. myoblasts; the expression of these factors diminishes once myogenic cells mature into myocytes and myotubes[39,43–50]. It is worth noting that myogenic cell morphology is dependent on the substrate they are cultured on. This is of importance if we want to infer cell phenotype based on morphology. Different coating solutions and different materials affect morphology, therefore it is important that these stages be identified at different institutions, and even within the same group, as they might differ from the ones presented here. Performing this initial analysis allowed

us to confirm our myogenic cultures were comparable to those of other groups[47,60,70]. Defining these morphological stages and comparing them with myogenic factor expression allowed us to quicky estimate cell phenotype based on morphological appearance and make efficient decisions about their culture, such as passaging cells if some have started to mature. Further exploration of the correlation between cell morphology and phenotype would involve finding a suitable measurement methodology for cell morphology and identifying how transcription factor expression correlates to those measurements. During transcription factor labeling, the use of control stains was employed to ensure the correct identification of the cells and avoid any bleedthrough effects from the different fluorophores. While the initial control stains were successful in confirming the results from our staining procedures, future studies would benefit from best practices during these assessments and include a control stain for every replicate to ensure the validity of the results. (**Figure S2** in **Appendix C** contains images of the control stains performed). Phenotyping using these procedures presented further challenges when cells were cultured on gelatin due to the inability to completely wash off the staining solution, which lead to noise during imaging and made quantification challenging.

Isolation Optimization

The first step of the optimization process involved improving the isolation of individual myofibers from Extensor Digitorum Longus (EDL) muscles. Changes to the initial protocol were gradually implemented and evaluated both qualitatively, through morphological assessment of cells, and quantitatively using cell number over time to determine the effectiveness of the isolated myofibers with respect to cell expansion. The biggest improvement in increasing the number of myofibers isolated came from using fresh collagenase II solution, which increased the amount of myofibers isolated by more than 100% when compared to frozen aliquots of collagenase II.

The mechanical separation and handling of myofibers was also critical for their viability; myofibers that were damaged during the transfer from the digesting flask to the culture flask

failed to yield SCs and reduced the effectiveness of the isolation protocol. Damaged and dead myofibers hypercontracted and failed to release SCs; in addition they also seemed to adversely affect the myofibers around them, potentially due to the release of apoptotic cytokines[73]. Gentle, consistent flushes of media were the best way to mechanically separate myofibers while maintaining their integrity, which required micropipettes to aspirate and eject consistent volumes of media. Periodic checks on the silicone adaptor seal used to connect the micropipette body to the glass tips ensured that the mechanical digestion and transport of myofibers was consistent between isolations. Regular maintenance of isolation equipment is critical to the success of the isolation procedure.

Changes in supplementation, from a 2ng/mL to a 10ng/mL dose of bFGF, and from a 5µM to 10µM dose of P38 inhibitor, increased the number of cells and decreased maturation, decreasing the time required for isolations to yield large numbers of proliferative myoblasts. The concentrations of these supplements were further evaluated to ensure the optimal concentrations were used.

Although the yield of myogenic cells was sufficient for *in vitro* studies and transplantation into preclinical mouse models, this isolation method presents potential problems for its translation into larger animal models and human use. The main drawback is the need for whole, undamaged myofibers to be isolated for SCs to migrate off the fibers and onto the flask. Even if we disregard potential rejection issues with transplanting donor cells, obtaining whole muscles and then isolating myofibers seems unlikely and would be increasingly complex as the size of the animal increases. To solve these potential issues, a bulk isolation method could be implemented. In general, bulk isolations can be more efficient at obtaining larger numbers of myoblasts than individual myofiber isolations, as the process of mechanically separating individual myofibers can be time consuming and result in lower yields when compared to bulk isolations[56,57]. However, individual myofiber isolations can produce higher purity myoblast

cultures, in theory, since the only cell type that would be able to migrate off the myofiber would be SCs[56]. The bulk isolation method involves mechanical and enzymatic digestion of minced muscle fragments to liberate single cells from the myofiber parenchyma and requires several pre-plating steps to remove unwanted cell types based on differences between adhesion times and adhesion strength[57]. This method quickly yields large numbers of myoblasts, making it ideal for obtaining a sufficient number of cells for transplantation without requiring whole muscles, and can be sourced from the recipient, circumventing rejection issues[34,56,57,74]. However, given the target population for this potential therapy, patients could present with preexisting conditions that impact the muscle and vascular tissue, which could present new problems, such as a diseased SC population that is unable to be expanded to sufficient quantities[41,51,56,66,75]. With regards to rejection, advances in biomaterials capable of avoiding an inflammatory response when transplanted could protect allogeneic SCs. Future studies could replace single myofiber isolation with bulk isolation and optimize this method to provide the same amount of undifferentiated myogenic cells as the myofiber isolation method. Diseased mouse models (suffering from PAOD or other diseases that this potential treatment could address) should also be explored to determine whether the cells isolated from this patient demographic have lower proliferative capacity and reduced potency[41,51,56,66,75].

In summary, the isolation method was optimized by modifying the enzymatic and mechanical digestion methods of the donor muscle, resulting in an isolation procedure capable of producing highly pure SC cultures. The subsequent aim involved exploring the effects of culturing myogenic cells in vitro and optimizing media supplementation to ensure the high purity of the isolated cells was not lost while maximizing their expansion.

Effects of Supplementation on Short and Long Term Culture

To determine the optimal media supplementation to maximize SC activation and myoblast expansion, we explored the effects of the supplements used during culture and their impact on

cell expansion and phenotype. The addition of bFGF and inhibiting p38 MAPK seemed to increase the number of immature myogenic cells.

To precisely determine their effect on myoblast proliferation and maturation, and SC migration from myofiber cultures, we measured the increase in cell number in response to different concentrations of bFGF and p38i. Cell expansion increased as bFGF concentration increased. Interestingly, no further increases in proliferation were observed when the bFGF concentration was doubled (10ng·mL$^{-1}$ to 20ng·mL$^{-1}$) (5.97 ± 0.50 to 6.83 ± 0.65). Inhibiting p38 MAPK had the opposite effect on cell expansion, decreasing cell expansion (5.97 ± 0.50 to 3.44 ± 0.29) when the standard dose was doubled (10µM to 20µM). These results seem align with those presented by other groups, which found that inhibition of p38 MAPK decreased cell expansion and did not recover with bFGF suplementation[59,64,70].

Although these results support the choice of supplement concentrations used in this study, there is still opportunity for further optimization. Specifically, the short culture time (72 hours) could explain why some groups are not significantly different. To test this hypothesis, multiple isolations would have to be performed, each one supplemented with different combinations of bFGF and p38i, and cultured for varying lengths of time. During the initial isolation optimization, cultures resulting from low numbers of myofibers (fewer than 50 per T12.5) stopped expanding and eventually began to die before reaching day 7, hence individual isolations would be needed to provide enough myofibers (more than 75) for long term expansion. We determined that three days was, on average, the longest a myofiber would 'release' SCs. This was determined from observations during culture, where myofibers would detach from the surface of the culture flask.

In summary, this study allowed us to determine that using a bFGF concentration of 10ng·mL$^{-1}$ and a 10µM concentration of SB 203580 maximized SC migration and initial expansion. To reach the required number of myogenic cells for transplantation, cells had to be

cultured for about 7 days, hence the effects of these supplements were evaluated for this longer time frame.

The role of bFGF and p38i on short term cultures (72 to 96 hours) has been previously investigated, however, little work has been caried out to evaluate the combination of both supplements in longer cultures (7+ days), specifically ones aimed at using them for the development of a cell therapy[58,59,68]. The latter consideration is critical since extended exposure to supplements could lead to unwanted effects on SC population (such as cell senescence) that could impact their secretion of growth factors, affecting the therapy's effectiveness[59]. Hence, the effect of each supplement separately, and the combination of both, was evaluated based on cell number and phenotype after 7 days in culture, as compared to a culture without any supplements. bFGF supplemented cultures had higher cell counts than those without; inhibiting p38 MAPK did not affect cell number. Cultures in which p38 MAPK was inhibited displayed higher MyoD expression than cultures without supplements; no other conditions affected MyoD expression. Neither supplementing bFGF nor inhibiting p38 MAPK affected Pax7 expression. The effect of bFGF on myoblast proliferation is consistent with previous findings[60,63]. bFGF also represses maturation of SCs by stimulating cyclin D1, which could explain why there was no difference between groups supplemented with bFGF and with inhibited p38 MAPK in both MyoD and Pax7 expression[61,63]. SCs cultured with this specific p38 inhibitor (SB 203580) failed to expand with changes in bFGF, preventing bFGF stimulated proliferation through the MAPK pathway[70]. If SB 203580 blocks bFGF induced cell proliferation, all groups supplemented with SB 203580 would have similar cell number counts to non-supplemented cultures and would have lower cell counts than bFGF only supplemented cultures. We observed cultures supplemented with both bFGF and SB 203580 had similar cell counts to cultures supplemented with just bFGF, suggesting bFGF was key in promoting cell proliferation and that p38i supplementation did not block its effect. Studies show p38 MAPK inhibition has no effect on bFGF induced increases in cyclin D1

through ERK signaling[68,81]. However, while bFGF signals through the ERK and p38 MAPK pathways, ERK activation alone is not sufficient for myoblast proliferation[68,81]. A possible explanation of these results would be that SB 203580 activity is time dependent. If SB 203580 no longer inhibited the P38 MAPK pathway after a certain time point, potentially due to a decrease in pharmacological activity (as it is used up, a behavior previously observed for other cell culture media supplements), bFGF could activate this pathway, increase cell expansion, and explain the results observed[76]. These previous studies mostly evaluate SC culture between 24 and 72 hours, which could explain why they observed no cell expansion with increases in bFGF following p38i supplementation (since p38i would still be active)[64,70]. However, it is worth mentioning these groups used higher concentrations (20µM in primary isolated SCs) than the ones used in this study and therefore further studies looking at the relationship between bFGF signaling and p38 MAPK inhibition could help clarify these results. A future study could look at the effects of these supplements more accurately by evaluating SB 203580 activity with time, specifically looking at inhibiting p38 MAPK at different stages of the culture (24 to 72 hours with no inhibition).

Mature cell types (those exhibiting no Pax7 or MyoD expression) are highly adherent and remain on the tissue culture flask during passaging. This property is beneficial to purify our cultures before transplantation and the dissociated cells are assessed and transplanted without further culture or passaging steps, hence our results are representative of the cells transplanted. However, this does affect the results (**Figure 6**), decreasing the number of non Pax7 or MyoD expressing cells and results in smaller differences between treatment groups. This does not fully reflect the effects of the p38i supplementation since the actual differences between groups are likely to be larger than the one illustrated in Figure 6. The importance of the p38i supplementation can be observed during the culture of myocytes where myoblast cultures quickly mature into myocytes without p38i supplementation (Figure 5B).

In summary, we validated the choice of media supplementation for extended cultures (more than 72 hours) which allowed us to obtain large numbers proliferating myoblasts. Once we had developed a robust method to obtain high yielding, high purity myoblast cultures, we began to assess the delivery vehicle selected. This included characterizing cells on the vehicle as well as determining their viability both pre- and post-transplantation.

Evaluation of the Gelatin Hydrogel Vehicle

Cell delivery strategies have been a highly researched subject in recent years as low retention rates limit the effectiveness of cell therapies, there is a <10% survival rate after 48h following direct injection of myoblasts into muscle[77–79]. Retention rate of cells refers to a quantitative assessment of the number of transplanted cells which remain in the target area over time. Different strategies include direct administration of cells in a buffer solution through injections and delivery using a vehicle such as a hydrogel carrier[80,81]. Strategies for cell delivery must be chosen with the proposed mode of action of the therapy in mind. For instance, a SC based therapy that aims to regenerate muscle tissue through cell engraftment would need a vehicle which allows for cells to fuse with native tissue. In the case of our therapy, strategies which maximize exposure (high retention rates) of the target area to the paracrine factors produced by SCs would be beneficial. Delivery strategies such as plating cells on injectable microscale cellular niches to transplant these into ischemic mouse models have been developed, reporting superior retention rates when compared to direct injection (96% on microscale niche versus 15% for direct injection) and leading to a significant improvement in blood perfusion[79,80,82]. Delivery using a vehicle such as a hydrogel carrier can result in higher retention rates than direct injection and are more easily fabricated when compared to complex delivery systems such as microscale cellular niches[80,81]. These studies demonstrate that delivery strategies are critical to a cell therapy's effectiveness.

To transplant viable cells in a reproducible manner, a gelatin hydrogel vehicle was used for its reproducibility and predictability. To evaluate the status of the cells on the vehicle, cell retention and phenotype were estimated through cell viability staining and Pax7 and MyoD transcription factor staining pre-transplantation and 7 days post-transplantation. Cell viability was 99% 12 hours after cell plating (pre-transplantation), but this number decreased dramatically to <1% at 7 days post-transplantation. Myoblasts were Pax7 and MyoD positive pre-transplantation (myocytes were negative for both) but there was no Pax7 or MyoD expression for any group at 7 days post-transplantation. Cell distribution after plating was inconsistent, with more cells adhering towards the center of the well. This led to inconsistent treatment dosages since the number of cells transplanted depended on the location where the transplant vehicle was punched out of the well. In the case that a hydrogel punch was removed from an area with fewer cells, it is possible that the effect of the cells in vivo would be diminished. The hydrogel was also difficult to transplant under the anterior gracilis in a limited space, often leading to friction on the surface of the hydrogel and possibly cells being removed from it. The drop in viability could be explained by the lack of nutrients reaching the cells on the construct and the potential friction on cells due to hindlimb movement. Cells in culture begin to differentiate soon after the cessation of bFGF supplementation and inhibition of p38 MAPK, so it is possible that the lack of Pax7 and MyoD expression could be due to myoblasts maturing. Myogenin staining could be used to identify mature myocytes to test this hypothesis. Interestingly, nuclear staining revealed cells present on the gelatin only vehicle, but live/dead staining revealed the same viability as with the other groups. A possible explanation could be an inflammatory response by the host, although gelatin displays a low inflammatory response, macrophages and other immune cells are attracted to the foreign body and generally attempt to encapsulate it[83–86]. This process can lead to potentially detrimental interactions between the host immune system and the transplanted cells, macrophages could encircle the construct or other immune cells could release cytotoxic cytokines, which could explain the low viability of cells 7 days post-transplantation and the presence of cells on the

gelatin-only vehicle. Although a gelatin hydrogel is effective in delivering cells to the target area, its effectiveness in maintaining their viability is not clear. The development of other vehicles, such as injectable thermorevesible polymers, can improve the delivery of cells by improving the ease of transplantation (removing the potential friction during implantation), increasing the number of cells transplanted (since they are not limited to the surface of the vehicle), and reducing foreign body response[83–86]. However, since cells will be embedded in the vehicle there could be an impact on oxygen supply to the cells and secreted growth factors could be trapped inside the vehicle.

We confirmed our ability to transplant viable myoblasts using the gelatin hydrogel vehicle and gained a better understanding on the behavior of these cells on the vehicle. The final stage of this thesis was to implement all of the previous aims into a pilot study similar to previous studies performed by our group.

Effects of Myoblast Transplantation on Collateral Arteriogenesis

Myoblasts and myocytes on gelatin hydrogel disks were transplanted under the gracilis muscle of BALB/c mice following femoral artery ligation. Neither myoblast nor myocyte transplantation enhanced collateral arteriogenesis. This result is similar to prior studies, which found no increases or inconsistent increases in collateral diameter after myoblast transplantation in lean C57Bl/6 mice[87]. However, myoblast transplantation did enhance collateral arteriogenesis in C57Bl/6 mice with DIO and collateral capillary arteriogenesis in the spinotrapezius muscle of BALB/c mice[52–54,88]. Additionally, neither myoblast nor myocyte transplantation affected collateral wall thickness. In addition to the limitations expressed above about potential issues with the gelatin hydrogel vehicle, the site of transplantation and mouse strain used could also explain this difference.  Previous studies explored the effects of myoblast transplantation in DIO C57Bl/6 under the gracilis muscle and in BALB/c mice under the spinotrapezius muscle, where collaterals form from capillaries undergoing arteriogenesis, forming arterialized capillary collaterals

(ACC)[52,54]. Studies looking at the impact of myoblast transplantation on arteriogenesis in DIO C57Bl/6 mice under the spinotrapezius muscle could show differences between implantation sites. Studies performed in DIO C57Bl/6 mice found an increase in collateral diameter after myoblast transplantation under the anterior gracilis[88]. This suggests that myoblast transplantation in BALB/c mice is not as effective in increasing collateral arteriogenesis compared to the same procedure in DIO C57Bl/6 mice. C57Bl/6 mice have extensive preexisting collateral circuits and are capable of robust collateral development, which is a contrast to BALB/c mice which have significantly fewer collateral circuits and display reduced collateral development and enlargement[89,90]. Even if DIO C57Bl/6 mice also display an impaired arteriogenic response (due to suppression of collateral growth), the difference in preexisting collateral circuits might explain the difference in experimental results between strains[91]. Although our group previously found myoblast transplantation promoted arteriogenesis in DIO C57Bl/6 mice but no impact in lean C57Bl/6 during this study, these differences could be explained by a reduced exposure of growth factors from transplanted myoblasts due to the low retention rate (evident from the low cell viability after transplantation during this study). The work done for this thesis could be used to determine whether these differences are due to differences in the transplanted cells. Further studies on the arteriogenic response of each mouse strain could aid in the selection of a suitable mouse model for future arteriogenesis studies.

Limitations

Technical limitations for the studies described herein that have not previously been described are related to study design. The time required for the isolation and culture of myoblasts, and the surgical procedures, lead to small replicate sizes (between n=2 and n=4 for the pilot study). This impacted the randomization of the study, which was limited to cell availability. A larger supply of animals for myogenic cell isolation and transplantation studies can help increase the number of replicates in these experiments, reducing some of the variability present.

Another important limitation lies in the complexity of immunofluorescent imaging, especially with regards to imaging on gelatin. Gelatin is autofluorescent, which made imaging cells on the gelatin hydrogels challenging by introducing noise in the form of bright light in the images taken. Another potential source of uncertainty during imaging was the material characteristics, specifically post-transplantation where the gelatin was in a more liquid state. During staining procedures, the lowered viscosity of the gelatin made it challenging to perform the necessary washing steps without aspirating the gelatin and could have trapped some of the immunofluorescent molecules, resulting in extremely bright fluorescent images. These issues resulted in potentially lower cell counts since some of the individual cells couldn't be discerned from the gelatin. The development of alternate transplantation vehicles mentioned above could help overcome these limitations and allow for more accurate cell counts on the vehicle.

Conclusion

Regardless of the outcome of the pilot study, the strategy implemented during this project provides a repeatable and complete framework to isolate, expand, and characterize myogenic cells to assess the cellular component of the proposed cell therapy. From our results, we propose the following framework to allow for more defined studies and easier comparison between studies. The development of a cell therapy in the proof-of-concept stage in small animal models involves four stages, cell isolation/sourcing, cell culture and expansion, vehicle development, and in vivo evaluation. At the end of each stage there must be a critical evaluation of the process and results obtained. After cell isolation/sourcing, the number of cells and their purity must be analyzed to determine if the selected method for obtaining cells matches the expectations for future steps. Once cells are obtained, we must evaluate the culture conditions and how these ensure optimal cell expansion to achieve the desired number of cells of the appropriate phenotype. This stage would involve determining proper media formulation to allow cells to expand to sufficiently large quantities while maintaining the desired phenotype. This step is a

critical addition to the previous procedure as it allows us to have more control over the in vitro expansion of these cells. After assessing the culture conditions, reliable cell transplantation strategies should be explored. Vehicle development is a critical stage that links the in vitro studies performed so far and the implementation of the therapy in vivo. Key evaluations during this stage involve interactions between the vehicle, cells, and animal subject. Here, we determined cell viability on the vehicle and cell survival through early in vivo studies before determining the effect of the therapy on collateral arteriogenesis. Material biocompatibility must also be assessed when implementing a new vehicle, including inflammatory response and cytotoxicity. Finally, the effects of the therapy in vivo can be evaluated. This stage involves the selection of a suitable animal model, both biological and surgical, and well-defined endpoints that best evaluate the desired clinical outcome. In the case of collateral arteriogenesis, a suitable mouse strain (which has preexisting collaterals) and ligation site should be considered first, followed by assessment of vascular response (through collateral enlargement, maturation, or innervation). Developing a reliable and wholistic process can help researchers determine potential bottlenecks in the development of the therapeutic candidate, and allow for appropriate resource allocation, which has become increasingly important as cellular therapy developments become increasingly expensive[92,93].

In summary, we developed a reliable procedure to isolate, expand, and characterize myogenic cells both during culture and on a gelatin hydrogel vehicle prior to performing a pilot study to evaluate the effects of this cell type on collateral arteriogenesis in a BALB/c hindlimb ischemic mouse model. Myogenic cell isolation, culture, and characterization were optimized to ensure a large population of proliferating myoblasts were obtained. These cells were then plated on a gelatin hydrogel where their phenotype was assessed to develop an effective method of transplanting them. The final step was to transplant them into the *in vivo* model and measure their effect on collateral arteriogenesis. The transplantation of myogenic cells did not enhance

collateral arteriogenesis. However, the whole process was successful in developing an optimized

methodology to isolate, culture, and assess myogenic cells in culture and on a gelatin hydrogel

vehicle, which resulted in a defined and reliable approach to be implemented in future studies.

# 5. REFERENCES

1.    Aronow WS. Peripheral arterial disease of the lower extremities. *Arch Med Sci*. 2012;8(2):375-388. doi:10.5114/aoms.2012.28568

2.    Boyd AM. Obstruction of the Lower Limb Arteries. *Proc R Soc Med*. 1962;55(7):591-599.

3.    Shu J, Santulli G. Update on peripheral artery disease: Epidemiology and evidence-based facts. *Atherosclerosis*. 2018;275:379-381. doi:10.1016/j.atherosclerosis.2018.05.033

4.    Criqui MH, Langer RD, Fronek A, et al. Mortality over a Period of 10 Years in Patients with Peripheral Arterial Disease. *New England Journal of Medicine*. 1992;326(6):381-386. doi:10.1056/NEJM199202063260605

5.    McDermott MM. Functional Impairment in Peripheral Artery Disease and How to Improve It in 2013. *Curr Cardiol Rep*. 2013;15(4):347. doi:10.1007/s11886-013-0347-5

6.    Hirsch AT, Criqui MH, Treat-Jacobson D, et al. Peripheral Arterial Disease Detection, Awareness, and Treatment in Primary Care. *JAMA*. 2001;286(11):1317-1324. doi:10.1001/jama.286.11.1317

7.    Jones WS, Dolor RJ, Hasselblad V, et al. Comparative effectiveness of endovascular and surgical revascularization for patients with peripheral artery disease and critical limb ischemia: Systematic review of revascularization in critical limb ischemia. *American Heart Journal*. 2014;167(4):489-498.e7. doi:10.1016/j.ahj.2013.12.012

8.    Phelps EA, Garcia AJ. Update on therapeutic vascularization strategies. *Regen Med*. 2009;4(1):65-80. doi:10.2217/17460751.4.1.65

9.    Adam DJ, Beard JD, Cleveland T, et al. Bypass versus angioplasty in severe ischaemia of the leg (BASIL): multicentre, randomised controlled trial. *The Lancet*. 2005;366(9501):1925-1934. doi:10.1016/S0140-6736(05)67704-5

10.   Epstein Stephen E., Lassance-Soares Roberta M., Faber James E., Burnett Mary Susan. Effects of Aging on the Collateral Circulation, and Therapeutic Implications. *Circulation*. 2012;125(25):3211-3219. doi:10.1161/CIRCULATIONAHA.111.079038

11.   van Royen N, Piek JJ, Schaper W, Fulton WF. A Critical Review of Clinical Arteriogenesis Research. *Journal of the American College of Cardiology*. 2009;55(1):17-25. doi:10.1016/j.jacc.2009.06.058

12.   Scholz D, Cai W, Schaper W. Arteriogenesis, a new concept of vascular adaptation in occlusive disease. :11.

13.   Chillo O, Kleinert EC, Lautz T, et al. Perivascular Mast Cells Govern Shear Stress-Induced Arteriogenesis by Orchestrating Leukocyte Function. *Cell Reports*. 2016;16(8):2197-2207. doi:10.1016/j.celrep.2016.07.040

14.   Heuslein JL, Meisner JK, Li X, et al. Mechanisms of Amplified Arteriogenesis in Collateral Artery Segments Exposed to Reversed Flow Direction. *Arterioscler Thromb Vasc Biol*. 2015;35(11):2354-2365. doi:10.1161/ATVBAHA.115.305775

15.  Losordo Douglas W., Dimmeler Stefanie. Therapeutic Angiogenesis and Vasculogenesis for Ischemic Disease. *Circulation*. 2004;109(21):2487-2491. doi:10.1161/01.CIR.0000128595.79378.FA

16.  Murrant CL, Sarelius IH. Local control of blood flow during active hyperaemia: what kinds of integration are important? *J Physiol*. 2015;593(21):4699-4711. doi:10.1113/JP270205

17.  Heil Matthias, Schaper Wolfgang. Influence of Mechanical, Cellular, and Molecular Factors on Collateral Artery Growth (Arteriogenesis). *Circulation Research*. 2004;95(5):449-458. doi:10.1161/01.RES.0000141145.78900.44

18.  Oostrom MC van, Oostrom O van, Quax PHA, Verhaar MC, Hoefer IE. Insights into mechanisms behind arteriogenesis: what does the future hold? *Journal of Leukocyte Biology*. 2008;84(6):1379-1391. doi:10.1189/jlb.0508281

19.  Hong H, Tian XY. The Role of Macrophages in Vascular Repair and Regeneration after Ischemic Injury. *Int J Mol Sci*. 2020;21(17). doi:10.3390/ijms21176328

20.  Dai X, Faber JE. Endothelial Nitric Oxide Synthase Deficiency Causes Collateral Vessel Rarefaction and Impairs Activation of a Cell Cycle Gene Network During Arteriogenesis. *Circ Res*. 2010;106(12):1870-1881. doi:10.1161/CIRCRESAHA.109.212746

21.  Wang S, Zhang H, Wiltshire T, Sealock R, Faber JE. Genetic Dissection of the Canq1 Locus Governing Variation in Extent of the Collateral Circulation. *PLOS ONE*. 2012;7(3):e31910. doi:10.1371/journal.pone.0031910

22.  Chalothorn D, Faber JE. Strain-dependent variation in collateral circulatory function in mouse hindlimb. *Physiological Genomics*. 2010;42(3):469-479. doi:10.1152/physiolgenomics.00070.2010

23.  Zhang Z, Slobodianski A, Ito WD, et al. Enhanced Collateral Growth by Double Transplantation of Gene-Nucleofected Fibroblasts in Ischemic Hindlimb of Rats. *PLOS ONE*. 2011;6(4):e19192. doi:10.1371/journal.pone.0019192

24.  Cuende N, Rico L, Herrera C. Concise Review: Bone Marrow Mononuclear Cells for the Treatment of Ischemic Syndromes: Medicinal Product or Cell Transplantation? *Stem Cells Transl Med*. 2012;1(5):403-408. doi:10.5966/sctm.2011-0064

25.  Wang J, Yu L, Jiang C, Chen M, Ou C, Wang J. Bone marrow mononuclear cells exert long-term neuroprotection in a rat model of ischemic stroke by promoting arteriogenesis and angiogenesis. *Brain Behav Immun*. 2013;0:56-66. doi:10.1016/j.bbi.2013.07.010

26.  Hao Q, Su H, Palmer D, et al. Bone Marrow-Derived Cells Contribute to VEGF-Induced Angiogenesis in the Adult Mouse Brain by Supplying MMP-9. *Stroke*. 2011;42(2):453-458. doi:10.1161/STROKEAHA.110.596452

27.  Walter Dirk H., Krankenberg Hans, Balzer Jörn O., et al. Intraarterial Administration of Bone Marrow Mononuclear Cells in Patients With Critical Limb Ischemia. *Circulation: Cardiovascular Interventions*. 2011;4(1):26-37. doi:10.1161/CIRCINTERVENTIONS.110.958348

28. Lin C-S, Lue TF. Defining Vascular Stem Cells. *Stem Cells Dev*. 2013;22(7):1018-1026. doi:10.1089/scd.2012.0504

29. Watt SM, Gullo F, van der Garde M, et al. The angiogenic properties of mesenchymal stem/stromal cells and their therapeutic potential. *Br Med Bull*. 2013;108(1):25-53. doi:10.1093/bmb/ldt031

30. Watt SM, Athanassopoulos A, Harris AL, Tsaknakis G. Human endothelial stem/progenitor cells, angiogenic factors and vascular repair. *J R Soc Interface*. 2010;7(Suppl 6):S731-S751. doi:10.1098/rsif.2010.0377.focus

31. Zakrzewski W, Dobrzyński M, Szymonowicz M, Rybak Z. Stem cells: past, present, and future. *Stem Cell Research & Therapy*. 2019;10(1):68. doi:10.1186/s13287-019-1165-5

32. Karantalis V, Balkan W, Schulman IH, Hatzistergos KE, Hare JM. Cell-based therapy for prevention and reversal of myocardial remodeling. *Am J Physiol Heart Circ Physiol*. 2012;303(3):H256-H270. doi:10.1152/ajpheart.00221.2012

33. Compagna R, Amato B, Massa S, et al. Cell Therapy in Patients with Critical Limb Ischemia. Stem Cells International. doi:https://doi.org/10.1155/2015/931420

34. Pagani FD, DerSimonian H, Zawadzka A, et al. Autologous skeletal myoblasts transplanted to ischemia-damaged myocardium in humans: Histological analysis of cell survival and differentiation. *Journal of the American College of Cardiology*. 2003;41(5):879-888. doi:10.1016/S0735-1097(03)00081-0

35. Tedesco FS, Dellavalle A, Diaz-Manera J, Messina G, Cossu G. Repairing skeletal muscle: regenerative potential of skeletal muscle stem cells. *J Clin Invest*. 2010;120(1):11-19. doi:10.1172/JCI40373

36. Bareja A, Billin AN. Satellite cell therapy – from mice to men. *Skelet Muscle*. 2013;3:2. doi:10.1186/2044-5040-3-2

37. Ciciliot S, Schiaffino S. Regeneration of Mammalian Skeletal Muscle: Basic Mechanisms and Clinical Implications. *CPD*. 2010;16(8):906-914. doi:10.2174/138161210790883453

38. Caron L, Kher D, Lee KL, et al. A Human Pluripotent Stem Cell Model of Facioscapulohumeral Muscular Dystrophy-Affected Skeletal Muscles. *STEM CELLS Translational Medicine*. 2016;5(9):1145-1161. doi:10.5966/sctm.2015-0224

39. Yin H, Price F, Rudnicki MA. Satellite Cells and the Muscle Stem Cell Niche. *Physiol Rev*. 2013;93(1):23-67. doi:10.1152/physrev.00043.2011

40. Lieber RL. *Skeletal Muscle Structure, Function, and Plasticity*. Lippincott Williams & Wilkins; 2002.

41. Mukund K, Subramaniam S. Skeletal muscle: A review of molecular structure and function, in health and disease. *Wiley Interdiscip Rev Syst Biol Med*. 2020;12(1). doi:10.1002/wsbm.1462

42. Arends F, Lieleg O. Biophysical Properties of the Basal Lamina: A Highly Selective Extracellular Matrix. *Composition and Function of the Extracellular Matrix in the Human Body*. Published online June 15, 2016. doi:10.5772/62519

43. Mauro A. SATELLITE CELL OF SKELETAL MUSCLE FIBERS. *J Biophys Biochem Cytol*. 1961;9(2):493-495.

44. Chagastelles PC, Nardi NB. Biology of stem cells: an overview. *Kidney Int Suppl (2011)*. 2011;1(3):63-67. doi:10.1038/kisup.2011.15

45. Dayanidhi S, Lieber RL. Skeletal muscle satellite cells: Mediators of muscle growth during development and implications for developmental disorders. *Muscle Nerve*. 2014;50(5):723-732. doi:10.1002/mus.24441

46. Olguín HC, Pisconti A. Marking the tempo for myogenesis: Pax7 and the regulation of muscle stem cell fate decisions. *J Cell Mol Med*. 2012;16(5):1013-1025. doi:10.1111/j.1582-4934.2011.01348.x

47. Chal J, Pourquié O. Making muscle: skeletal myogenesis *in vivo* and *in vitro*. *Development*. 2017;144(12):2104-2122. doi:10.1242/dev.151035

48. Chal J, Oginuma M, Al Tanoury Z, et al. Differentiation of pluripotent stem cells to muscle fiber to model Duchenne muscular dystrophy. *Nat Biotechnol*. 2015;33(9):962-969. doi:10.1038/nbt.3297

49. Chal J, Al Tanoury Z, Oginuma M, et al. Recapitulating early development of mouse musculoskeletal precursors of the paraxial mesoderm *in vitro*. *Development*. 2018;145(6):dev157339. doi:10.1242/dev.157339

50. Zammit PS, Relaix F, Nagata Y, et al. Pax7 and myogenic progression in skeletal muscle satellite cells. *Journal of Cell Science*. 2006;119(9):1824-1832. doi:10.1242/jcs.02908

51. Dumont NA, Wang YX, Rudnicki MA. Intrinsic and extrinsic mechanisms regulating satellite cell function. *Development*. 2015;142(9):1572-1581. doi:10.1242/dev.114223

52. Hamzeinejad V, Banuelos L, Cardinal TR. Myoblasts enhance collateral capillary arteriogenesis during chronic ischemia. *The FASEB Journal*. 2018;32(S1):710.9-710.9. doi:10.1096/fasebj.2018.32.1_supplement.710.9

53. Go J. Influence of Myoblasts on Arteriogenesis in a Murine Chronic Hindlimb Ischemia Model. Published online June 2014. Accessed October 10, 2020. https://content-calpoly-edu.s3.amazonaws.com/bmed/1/images/Go_Jennifer_Applications_Report.pdf

54. Hamzeinejad V. IMPACT OF MYOBLAST TRANSPLNATATION ON FUNCTIONAL VASODILATION IN BALB/C SPINOTRAPEZIUS MUSCLE. Published online August 2017.

55. Malliaras K, Marbán E. Cardiac cell therapy: where we've been, where we are, and where we should be headed. *Br Med Bull*. 2011;98(1):161-185. doi:10.1093/bmb/ldr018

56. Shefer G, Van de Mark DP, Richardson JB, Yablonka-Reuveni Z. Satellite-cell pool size does matter: defining the myogenic potency of aging skeletal muscle. *Dev Biol*. 2006;294(1):50-66. doi:10.1016/j.ydbio.2006.02.022

57. Hindi L, McMillan J, Afroze D, Hindi S, Kumar A. Isolation, Culturing, and Differentiation of Primary Myoblasts from Skeletal Muscle of Adult Mice. *BIO-PROTOCOL*. 2017;7(9). doi:10.21769/BioProtoc.2248

58. Cuenda A, Rouse J, Doza YN, et al. SB 203580 is a specific inhibitor of a MAP kinase homologue which is stimulated by cellular stresses and interleukin-1. *FEBS Letters*. 1995;364(2):229-233. doi:10.1016/0014-5793(95)00357-F

59. Davies SP, Reddy H, Caivano M, Cohen P. Specificity and mechanism of action of some commonly used protein kinase inhibitors. *Biochem J*. 2000;351(Pt 1):95-105.

60. Rao SS, Kohtz DS. Positive and Negative Regulation of D-type Cyclin Expression in Skeletal Myoblasts by Basic Fibroblast Growth Factor and Transforming Growth Factor β A ROLE FOR CYCLIN D1 IN CONTROL OF MYOBLAST DIFFERENTIATION. *J Biol Chem*. 1995;270(8):4093-4100. doi:10.1074/jbc.270.8.4093

61. Clegg CH, Linkhart TA, Olwin BB, Hauschka SD. Growth factor control of skeletal muscle differentiation: commitment to terminal differentiation occurs in G1 phase and is repressed by fibroblast growth factor. *J Cell Biol*. 1987;105(2):949-956.

62. Itoh N, Mima T, Mikawa T. Loss of fibroblast growth factor receptors is necessary for terminal differentiation of embryonic limb muscle. :10.

63. Baldin V, Lukas J, Marcote MJ, Pagano M, Draetta G. Cyclin D1 is a nuclear protein required for cell cycle progression in G1. *Genes Dev*. 1993;7(5):812-821. doi:10.1101/gad.7.5.812

64. Jones NC, Fedorov YV, Rosenthal RS, Olwin BB. ERK1/2 is required for myoblast proliferation but is dispensable for muscle gene expression and cell fusion. *Journal of Cellular Physiology*. 2001;186(1):104-115. doi:10.1002/1097-4652(200101)186:1<104::AID-JCP1015>3.0.CO;2-0

65. Cornelison DDW, Wilcox-Adelman SA, Goetinck PF, Rauvala H, Rapraeger AC, Olwin BB. Essential and separable roles for Syndecan-3 and Syndecan-4 in skeletal muscle development and regeneration. *Genes Dev*. 2004;18(18):2231-2236. doi:10.1101/gad.1214204

66. Baj A, Bettaccini AA, Casalone R, Sala A, Cherubino P, Toniolo AQ. Culture of skeletal myoblasts from human donors aged over 40 years: dynamics of cell growth and expression of differentiation markers. *J Transl Med*. 2005;3:21. doi:10.1186/1479-5876-3-21

67. Charville GW, Cheung TH, Yoo B, et al. Ex Vivo Expansion and In Vivo Self-Renewal of Human Muscle Stem Cells. *Stem Cell Reports*. 2015;5(4):621-632. doi:10.1016/j.stemcr.2015.08.004

68. Ornatsky OI, Cox DM, Tangirala P, et al. Post-translational control of the MEF2A transcriptional regulatory protein. *Nucleic Acids Res*. 1999;27(13):2646-2654.

69. Emerson C, Sweeney HL. *Methods in Muscle Biology*. Academic Press; 1997.

70. Jones NC, Tyner KJ, Nibarger L, et al. The p38α/β MAPK functions as a molecular switch to activate the quiescent satellite cell. *J Cell Biol*. 2005;169(1):105-116. doi:10.1083/jcb.200408066

71. Tietze EM. ISOLATION AND CULTURE OF MYOFIBER-DERIVED CELLS FROM THE EXTENSOR DIGITORUM LONGUS MUSCLE. Published online February 2016.

72. Wierzbinski KR, Szymanski T, Rozwadowska N, et al. Potential use of superparamagnetic iron oxide nanoparticles for in vitro and in vivo bioimaging of human myoblasts. *Scientific Reports*. 2018;8(1):3682. doi:10.1038/s41598-018-22018-0

73. Tidball JG. Inflammatory processes in muscle injury and repair. *American Journal of Physiology-Regulatory, Integrative and Comparative Physiology*. 2005;288(2):R345-R353. doi:10.1152/ajpregu.00454.2004

74. Jarocha D, Stangel-Wojcikiewicz K, Basta A, Majka M. Efficient myoblast expansion for regenerative medicine use. *International Journal of Molecular Medicine*. 2014;34(1):83-91. doi:10.3892/ijmm.2014.1763

75. Jv C, Km J, Ma B, As B. The aged niche disrupts muscle stem cell quiescence. *Nature*. 2012;490(7420):355-360. doi:10.1038/nature11438

76. Ghanemi A. Cell cultures in drug development: Applications, challenges and limitations. *Saudi Pharm J*. 2015;23(4):453-454. doi:10.1016/j.jsps.2014.04.002

77. Aicher Alexandra, Brenner Winfried, Zuhayra Maaz, et al. Assessment of the Tissue Distribution of Transplanted Human Endothelial Progenitor Cells by Radioactive Labeling. *Circulation*. 2003;107(16):2134-2139. doi:10.1161/01.CIR.0000062649.63838.C9

78. Hou Dongming, Youssef Eyas Al-Shaykh, Brinton Todd J., et al. Radiolabeled Cell Distribution After Intramyocardial, Intracoronary, and Interstitial Retrograde Coronary Venous Delivery. *Circulation*. 2005;112(9_supplement):I-150. doi:10.1161/CIRCULATIONAHA.104.526749

79. Qu Z, Balkir L, van Deutekom JCT, Robbins PD, Pruchnic R, Huard J. Development of Approaches to Improve Cell Survival in Myoblast Transfer Therapy. *J Cell Biol*. 1998;142(5):1257-1267.

80. Li Y, Liu W, Liu F, et al. Primed 3D injectable microniches enabling low-dosage cell therapy for critical limb ischemia. *Proc Natl Acad Sci U S A*. 2014;111(37):13511-13516. doi:10.1073/pnas.1411295111

81. Ifkovits JL, Tous E, Minakawa M, et al. Injectable hydrogel properties influence infarct expansion and extent of postinfarction left ventricular remodeling in an ovine model. *Proc Natl Acad Sci U S A*. 2010;107(25):11507-11512. doi:10.1073/pnas.1004097107

82. MacAskill MG, Saif J, Condie A, et al. Robust Revascularization in Models of Limb Ischemia Using a Clinically Translatable Human Stem Cell-Derived Endothelial Cell Product. *Molecular Therapy*. 2018;26(7):1669-1684. doi:10.1016/j.ymthe.2018.03.017

83. Marquardt LM, Heilshorn SC. Design of Injectable Materials to Improve Stem Cell Transplantation. *Curr Stem Cell Rep*. 2016;2(3):207-220. doi:10.1007/s40778-016-0058-0

84. Park J, Baranov P, Aydin A, et al. In Situ Cross-linking Hydrogel as a Vehicle for Retinal Progenitor Cell Transplantation. *Cell Transplant*. 2019;28(5):596-606. doi:10.1177/0963689719825614

85. Celikkin N, Rinoldi C, Costantini M, Trombetta M, Rainer A, Święszkowski W. Naturally derived proteins and glycosaminoglycan scaffolds for tissue engineering applications. *Materials Science and Engineering: C*. 2017;78:1277-1299. doi:10.1016/j.msec.2017.04.016

86. Anderson JM, Rodriguez A, Chang DT. FOREIGN BODY REACTION TO BIOMATERIALS. *Semin Immunol*. 2008;20(2):86-100. doi:10.1016/j.smim.2007.11.004

87. Sivesind PM. The Impacts of Sex and Myogenic Cell Transplantation on Collateral Capillary Arteriogenesis. Published online March 1, 2018. doi:10.15368/theses.2018.8

88. Tran CM, Hamzeinejad V, Cardinal TR. The Impact of Primary Myoblast Transplantation on Functional Vasodilation Following Arteriogenesis in Mice with Diet-Induced Obesity. *The FASEB Journal*. 2018;32(S1):573.10-573.10. doi:https://doi.org/10.1096/fasebj.2018.32.1_supplement.573.10

89. Collinson DJ, Donnelly R. Therapeutic Angiogenesis in Peripheral Arterial Disease: Can Biotechnology Produce an Effective Collateral Circulation? *European Journal of Vascular and Endovascular Surgery*. 2004;28(1):9-23. doi:10.1016/j.ejvs.2004.03.021

90. McClung JM, McCord TJ, Keum S, et al. Skeletal Muscle–Specific Genetic Determinants Contribute to the Differential Strain-Dependent Effects of Hindlimb Ischemia in Mice. *Am J Pathol*. 2012;180(5):2156-2169. doi:10.1016/j.ajpath.2012.01.032

91. DiStasi MR, Mund JA, Bohlen HG, et al. Impaired compensation to femoral artery ligation in diet-induced obese mice is primarily mediated via suppression of collateral growth by Nox2 and p47phox. *Am J Physiol Heart Circ Physiol*. 2015;309(7):H1207-H1217. doi:10.1152/ajpheart.00180.2015

92. Cell Therapy Market Size | Industry Growth Report, 2020-2027. Accessed August 25, 2020. https://www.grandviewresearch.com/industry-analysis/cell-therapy-market

93. State-of-the-Industry-2019-FINAL.pdf. Accessed August 25, 2020. https://alliancerm.org/wp-content/uploads/2019/01/State-of-the-Industry-2019-FINAL.pdf

# 6. APPENDICES

## A. Experimental Protocols

**Myofiber Isolation**

Date: _____

**Purpose**
To excise whole mouse Extensor Digitorum Longus (EDL) muscles, isolate individual live myofibers from whole muscles, and plate live myofibers in culture conditions to facilitate the primary culture of myoblasts.

**Necessary Material**

- Wash media (10% FBS in Base Media)
- Base media (1% Pen-Strep in HAMs F10)
- Growth media (20% FBS in Base Media)
- SB 203580 working solution (5 mM)
- bFGF working solution (1μg/mL)
- Collagenase II solution (2mg/mL)
- Horse Serum (HS)
- ECM coating solution (1:100)
- 18 MΩ Water
- T 12.5 flask (cell culture treated)
- 10 cm TC dishes (x5)
- 15 mL conical tubes

- Sterile Filter System
- Sterile PBS (1x)
- P1000 micropipette aid and tips
- P20 micropipette aid and tips
- Standard pattern forceps
- Curved iris scissors
- 5/45 Forceps (x2)
- Beveled long bore glass pipettes
- Cotton swabs
- 2x2, 4x4 gauze pads
- Isopropyl Alcohol (IPA)
- Styrofoam working surface

**Mouse Information**
Age: _____(3-4 week)
Sex:_____
Weight:_____
Genotype:_____

**TC Dish Preparation**
1. ___ Coat a T12.5 with 0.5 mL ECM coating
2. ___ Allow final plate to coat overnight on rocking platform (~ 10 rpm)
3. ___ In the morning wash plate with sterile PBS
   a. 10 minutes per wash on rocking platform (~ 10 rpm)
   b. 2 washes
   c. Wash with wash media (Sterile filter media)

**Collagenase Incubation Solution**
1. ___ Weigh out 6 mg of type II collagenase
2. ___ In BSC combine with 3 mL of Base Media
3. ___ Resuspend well

**Muscle Fiber Wash Plates**
1. ___ Defrost aliquot of HS
2. ___ In BSC, Coat 4x 10cm dishes in HS
   a. Label TC dishes 1-4
   b. Pipette 7 mL of HS into first 10 cm dish
   c. Transfer HS between dishes
   d. Place remaining HS in 15 mL conical and place in 37°C water bath

   e. Aspirate excess HS from TC dishes
3. ___ Place 15 mL of wash media into Dish 1
4. ___Place 5 mL of wash media into Dishes 2-4
5. ___ Warm plates in 37°C, 5% CO$_2$ incubator

**Muscle Excision – Extensor Digitorum Longus (EDL)**
1. ___ Euthanize mouse
2. ___ Use insulin syringe needles to secure fore and hind limbs to Styrofoam working surface
3. ___Thoroughly spray hindlimbs with IPA
4. ___Carefully remove the skin of both hindlimbs
   a. The hindlimb should be exposed from the knee joint to the midpoint of each foot
5. ___ Carefully remove connective tissue around the Tibialis Anterior (TA) Muscle
   a. Make sure to expose the origin of the EDL at the knee
6. ___ Create a pocket deep to the distal TA tendon below the ankle
7. ___ Cut the distal TA tendon
8. ___ Holding the TA by its distal tendon, pull it towards the knee cutting away connective tissue as needed to separate it from the EDL

54

1. ___ Cut the TA at its origin and set aside to expose the EDL
2. ___ Create a pocket deep to the distal EDL tendon
3. ___ Cut the Distal EDL tendon
4. ___ Holding the cut tendon, carefully pull EDL towards the knee separating it from the surrounding tissue
   a. Avoid stretching the muscle as it will damage individual myofibers
5. ___ Cut the proximal EDL tendon
   a. Tendon to Tendon isolation is critical to maintain fiber integrity
6. ___ Place EDL muscle into 3.0 mL of collagenase solution
7. ___ Repeat process for contralateral hindlimb
   a. placing muscles in collagenase solution more than 5 min apart will lead to uneven digestion

**Muscle Digestion**
1. ___ Place 15 mL conical with EDL muscles and collagenase in 37$^o$C water bath
2. ___ Repeatedly invert the 15 mL conical for every 10 min of incubation
3. ___ Incubate for 10 min
   a. Digestion can take between 10-30 min depending upon collagenase activity
4. ___ Following 10 min, remove 15 mL conical every 5-10 min and inspect for proper digestion
   a. Use dissecting microscope light on brightest setting for lighting
   b. When properly digested individual myofibers should begin to protrude from the surface of the muscle belly
   c. If the muscle appears fuzzy under a dissecting microscope or individual fibers appear fat and milky in color, the muscle has been overdigested
5. ___ Upon proper digestion level, remove 15 mL conicals with HS and muscles from the water bath
6. ___ Spray conicals down with IPA
7. ___ Remove dish 1 from incubator

8. ___ Coat glass pipettes in HS
9. ___ Use glass pipettes to remove muscles from the 15 mL conical and transfer into the first dish
   a. Place both muscles into the first dish
   b. Place collagenase solution back into the water bath (in case further digestion is needed)
10. ___ Use glass pipettes to dissociate muscles
   a. Progressively use smaller bevel pipettes as the muscle becomes more dissociated
   b. The muscle should only be washed with media or gently pipetted up and down
11. ___ Coat P1000 pipette tips with HS
12. ___ Use a dissecting scope and P1000 pipette to pick out individual live myofibers from the dish
   a. Live myofibers will appear shiny or clear and be straight or crinkly
   b. Dead myofibers will appear opaque and bent or short
13. ___ Place all live fibers in the next numbered dish
   a. Muscles should not remain out of the incubator for more than 10 min
14. ___ Repeat transfer process for the other wash dishes
15. ___ Transfer fibers as described into the ECM coated dish
16. ___ In a BSC, add 2 μL bFGF solution per 1mL of media
17. ___ In a BSC, add 2 μL P38 inhibitor solution (5mM) per 1mL of media
18. ___ Place final dish back in the incubator
   a. Myoblasts should begin to migrate from the myofibers within 3 days
   b. Feed after 5 days (Partial media change performed by transferring old media into a conical with 5mL of fresh warm media and transferring 5mL of the solution into the flask)
19. ___ Passage cells upon local confluence or average 80% confluence

NOTES:
- EDL muscles will have individual fibers protruding from the surface and slightly separate in the body of the muscle when properly digested
- The use of a wash dish (dish 4) is only necessary if a large number of dead or fragments of fibers are impeding the aspiration of live fibers only. You only want to aspirate live fibers
- Cells should be passed when large, dense (80% confluent) colonies appear around fibers. If cells start to elongate (starting to differentiate), they should also be passed

**Primary Myoblast Expansion Protocol**

Date:_____

**Purpose:** To expand primary mouse myoblasts from live Extensor Digitorum (EDL) muscle fibers

**Necessary Materials:**
- Growth Media (20% FBS in Base Media)
- SB 203580 working solution (5 mM)
- bFGF working solution (1μg/ml in PBS)
- Cell Dissociation Solution - EDTA (Fisher 13151014)
- PBS (-/-, $Ca^{+2}$, $Mg^{+2}$)
- ECM coated flask
- Microvial
- Hemocytometer

1. ___ Obtain an ~80% confluent culture vessel
   a. myoblasts will begin to differentiate and form myotubes as they approach confluency
   b. Takes up to 8 days before they are ready to pass
2. ___ Clean Phase Contrast Microscope with 70% v/v Isopropanol (IPA)
3. ___ Image save pictures of the culture with a phase contrast microscope
4. ___ Determine passage ratio to be used
   a. myoblasts should not be split at a ratio higher than 1:3

**EDTA Passaging**
1. ___ Warm Growth media and factors in 37C $H_2O$ bath immediately before use
2. ___ Aspirate media from culture vessel
3. ___ Wash with DPBS (-/-) and aspirate (repeat 2x)
4. ___ Add warm Cell Dissociation solution
   a. 0.066 ml/cm$^2$ surface (T12.5 – 0.8 ml, T75 – 5 ml)
5. ___ Immediately place in incubator for ~5 min
6. ___ Observe with phase contrast microscope
   a. cells should begin to ball up and become phase bright
7. ___ Hit the flask repeatedly to dislodge weakly adherent cells
   a. more differentiated cells will more strongly adhere to the dish
8. ___ If insufficient cells have detached, return to the incubator for an additional min
9. ___ Repeat process until sufficient cells have detached
   a. highly differentiated cells may never detach
   b. cells can be selectively passaged by altering incubation time/hitting of the flask
10. ___ Add the same volume of Growth Media as EDTA to prevent further chelation
11. ___ Label a 15 ml conical tube and transfer the cell suspension
12. ___ Count cells using hemocytometer
13. ___ Centrifuge at 300g for 5 min to create a cell pellet
14. ___ Aspirate media from the conical
   a. be careful to avoid aspirating the pellet
15. ___ Resuspend in the volume of growth media (+ factors) appropriate for the chosen passage ratio
16. ___ Repeatedly pipette up and down to break of cell clumps
17. ___ Rock the culture vessel repeatedly: forward/back and left/right to evenly disperse the cells
   a. Even cell distribution can be checked under the phase contrast microscope
18. ___ Place in incubator
   a. close the door gently to prevent uneven cell distribution

**Myoblast Antibody Staining**

Date: _____

**Purpose:**
To fix and stain myoblasts using antibody stains in order to assess their phenotype

**Necessary Materials**
- 8 Well Chamber Slide
- ECM Coating
- 4% Paraformaldehyde
- PBS
- Aluminum Foil

- UltraCruz Blocking Reagent
- Triton X-100
- Primary Conjugated Antibodies
- Mounting Medium (W/ DAPI)

**Slide prep, fixation, and solution prep**
1. ___ In a Biological Safety Cabinet (BSC) coat 8 Well Chamber Slide with ECM coating
    a. 0.2 mL per well
    b. Coat on rocking platform (10 rpm) for either:
        i. 3 hours at RT
        ii. overnight at RT
2. ___ Aspirate Coating
3. ___ Wash twice in PBS for 10 min
4. ___ Add $6 \times 10^4$ cells per well diluted in 0.5 mL of media
5. ___ Incubate until cells adhere (12-24 hours)
6. ___ Aspirate media and fix in 4% Paraformaldehyde at room temperature for 10 minutes (enough to cover surface)
7. ___ Aspirate PBS and wash twice in PBS and store in PBS (0.2 mL)
    a. Fixed cells can be stored prior to staining for up to 10 days
8. ___ Prepare permeabilization solution: 0.5% Triton X-100 in PBS
9. ___ Primary Conjugated Antibodies (1:200 MyoD, 1:100 PAX7) diluted in UltraCruz Blocking reagent

**Staining**
1. ___ Wash three times in PBS
2. ___ Aspirate PBS and add permeabilization solution for 5 minutes
3. ___ Aspirate permeabilization solution and add blocking solution for 30 minutes
4. ___ Wash in PBS for 5 minutes
5. ___ Incubate primary conjugated antibody solution at room temperature in the dark for 60 minutes
6. ___ Aspirate primary conjugated antibody solution wash three times in PBS for 5 minutes each
7. ___ Mount coverslip with mounting medium containing DAPI

**Sterile Gelatin Preparation**

Date:_____

**Sterile Materials**
- 25ml Erlenmeyer flask
- Rubber stopper + tubing
- Rubber stopper
- Spatula
- Distilled $H_2O$
- Gelatin powder

- 10mL syringe
- Syringe filter
- Pipettes
- 50 mL conicals
- 24 Well Plate

**Non-Sterile Materials**
- Hot plate
- Analytical balance
- 6mM EDC in DI-water

**Procedure**

___Turn hot plate on to 200°C.

___In laminar flow hood, open sterile packs with Erlenmeyer flask and rubber stopper.

___Weigh empty 25ml Erlenmeyer flask + rubber stopper on an analytical balance and zero the balance.

___Bring the Erlenmeyer flask back to the hood along with the gelatin.

___Open the sterile pack with the spatula and use it to put some gelatin powder into the Erlenmeyer flask.

___Put the rubber stopper back on the flask and weigh it on the analytical balance.

___Add enough distilled $H_2O$ to the flask to make a 10% gelatin solution (by weight).

___Open the sterile pack with the rubber stopper + tubing and put it on the flask.

9. ___Place flask on the hot plate, wait to boil, and then allow it to boil for 5 minutes.

10. ___In the hood, put 0.25mL of the gelatin solution in each well of a 24 well plate.

11. ___While the gelatin in solidifying, use the syringe filters to filter the 6mM EDC.

12. ___Once the gelatin has solidified, add 0.5mL of EDC to each well.

13. ___Leave the gelatin in the EDC solution 48 hours at 4°C to allow for crosslinking.

14. ___The next day aspirate the EDC solution and wash the gel 3x30 minutes with sterile $H_2O$.

15. ___ Seed each well of with 0.5 mil Myoblast suspended in 1mL of wash media.

**Note:** The measurements and seeding densities are given for 24 well plate. They need be adjusted if different size well is used.

Date_____ **Hindlimb Ischemia Surgery – Femoral Artery Ligation** Initials_____

**Purpose:** Simulate arterial occlusion

**Materials**

Pre-sterilize in autoclave

____1. Standard pattern forceps (1)
____2. Fine forceps- S&T (2)
____3. Ultrafine forceps- 545 (1)
____4. Curved iris scissors (1)
____5. Microdissection scissors (1)
____6. Gauze sponges- 2x2 and 4x4
____7. Cotton swabs
____8. 6.0 silk suture (2 x 1-inch pieces)
____9. 7.0 prolene suture
____10. Needle holder (1)

Obtain in surgery suite

____11. Depilatory cream- Veet
____12. Non-sterile cotton swabs
____13. Non-sterile gauze sponges (2x2 and 4x4)
____14. Chlorhexidene diacetate (Nolvasan) to disinfect surgical site before incision
____15. 1-mL insulin syringes (2)
____16. Buprenorphine analgesic (0.03 mg·ml$^{-1}$)
____17. Ear punch
____18. Veterinary ointment, applied to corneas
____19. Surgical tape
____20. FST heat pad w/ rectal probe
____21. Surgical scrubs
____22. Sterile petri dish (1)
____23. Sterile 5-mL syringe (1)
____24. Sterile saline
____25. Isolation mask and cap
____26. Sterile gloves
____27. Recovery bin and heat pad
____28. 70% isopropyl alcohol (IPA) to disinfect stage, microscopes, stage

**Animal preparation**

____29. Spray surgery area with Nolvasan.
____30. Place animal in induction chamber.
____31. Open oxygen cylinder. Set flow high and isofluorane to 5%.
____32. Once anesthetized, weigh animal and move to preparatory bench in a supine position.
____33. Reduce isoflurane to 1-3% and flow to 0.5-1.5 l·min$^{-1}$.
____34. Gently apply veterinary ointment to eyes using a cotton swab.
____35. Apply depilatory cream to hindlimb with a cotton swab and let sit for 1-3 minutes.
____36. Spray a 2x2 gauze sponge with Nolvasan and wipe hindlimb clean of cream and hair.

____37. Flip animal over and apply ear punch to the skin, avoid cartilage.
____38. Administer pre-op buprenorphine dose (0.075 mg·kg$^{-1}$) by subcutaneous injection.
____39. Cover heat pad with a 4x4 gauze sponge and transfer animal to surgery stage.
____40. Apply lubricant to rectal probe and insert. Set thermo-controller to 35°C.
____41. Change into surgical scrubs and wash hands/forearms.
____42. Open sterile instrument tray and sterile pack.
____43. Obtain sterile petri dish in sterile field and fill with sterile saline, using a 5-mL syringe.
____44. Put on mask, cap, and position/focus microscope before putting on sterile gloves.

**Surgery**

____45. Make a small incision on the middle, medial aspect of the left hindlimb, directly over the neurovascular bundle.
____46. Extend incision to the abdominal wall, reaching the fat pad
____47. Blunt dissect subcutaneous connective tissue to maximize surgical exposure.
____48. Blunt dissect and retract epigastric fat pad to expose ligation site, proximal to the popliteal artery and distal to the epigastric.
____49. Blunt dissect connective tissue over bundle and separate nerve from the artery-vein pair.
____50. Use ultrafine forceps to separate the artery from the vein.
____51. Tie off the femoral artery with silk suture.
____52. Use 7-0 prolene suture to close the incision with spiral sutures.
____53. Make a small incision in the middle medial aspect of the left hindlimb.
____54. Extend incision to the abdominal wall
____55. Blunt dissect subcutaneous connective tissue to maximize surgical exposure.
____56. Use 7-0 prolene suture to close the incision with spiral sutures.
____57. Repeat 53-56 on sham side, contralateral without artery/vein/nerve seperation

**Post-Surgical**

____58. Administer post-op buprenorphine dose (0.075 mg·kg$^{-1}$) by subcutaneous injection.
____59. Microwave recovery heat pad for ~1-2 min.
____60. Transfer animal to recovery a previously disinfected bin. Leave animal there until ambulatory.
____61. Turn off isoflurane, flow, and close oxygen.
____62. Wipe down surgical area with IPA and wash all instruments.

**Purpose**: To quantify the functionality of the gracilis collateral by measuring vessel dilation before and after electronically stimulating the muscle. It is important to quantify the response to increased metabolic demand because it provides a functional endpoint for assessing arteriogenesis.

**Safety Considerations**
- Avoid contact with the electrode during stimulation to avoid shock
- Handle surgical instruments delicately/with caution to avoid puncturing oneself or others

**Materials**
__1. Standard pattern forceps (1)
__2. Fine forceps- S&T (2)
__3. Sharp forceps- 5/45 (1)
__4. Curved iris scissors (1)
__5. Retractors (2)
__6. Depilatory cream- Veet
__7. Cotton Swabs
__8. Gauze Sponges (2x2 and 4x4)
__9. Lubricant for temperature probe
__10. Surgical tape
__11. Heat pad w/ rectal probe
__12. 10mL syringe (PBS sterilization)
__13. Syringe filter (PBS ster.)
__14. Saline (PBS)
__15. Tungsten microelectrodes (2xwidth)
__16. Clay
__17. Plastic wrap
__18. Stage w/ attached Cyan Trans-illuminators
__19. Intravital microscope- Olympus BXFM
__20. Digital imaging software- QCapturePro
__21. $10^{-[4-5]}$ sodium nitroprusside (SNP) at 37C (keep protected from light while thawing)
__22. $10^{-[4-5]}$ norepinephrine (NE)
__23. 70% isopropyl alcohol (IPA)

**Animal Preparation**
__24. Place animal in induction chamber
__25. Open oxygen cylinder. Set flow high and isofluorane to 5%
__26. Once anesthetized, weigh animal and move to preparatory bench in a supine position
__27. Reduce isofluorane to 1-3% and flow to 0.5-1.5 l*min^-1

__28. Apply a thick coating of depilatory cream to hindlimb with a cotton swab. Let sit for 1-3 minutes.
__29. Drywipe with enough force to remove the hair and cream w/o irritating the skin. Wet a 2x2 gauze sponge with PBS and wipe hindlimb clean of cream and hair
__30. Flip animal over and use clippers to shave hair from the posterior side of the hindlimbs
__31. Complete hair removal w/ depilatory cream
__32. Cover heat pad w/ 4x4 gauze sponge and transfer animal to surgery stage
__33. Apply lubricant to rectal probe and insert. Set thermo-controller to 35°C
__34. Tape hindlimb flat, as perfectly horizontal in same plane as stage, as possible over LED

**Surgical Exposure**
__35. Make a small incision on the middle, medial aspect of the left hindlimb
__36. Continue to make a circular incision from the saphenous to the epigastric fat pad
__37. Remove just enough skin to create "a bowl" for the PBS
__38. Blunt dissect and remove the connective tissue overlying the gricilis muscle
__39. Remove the construct from the pocket deep to the gracilis muscle. Place construct in PBS.
__40. Remove skin from the back of hindlimb and cover with plastic wrap? (if necessary)
__41. Set frequency to 1 Hz (1000ms pulse interval), the duration to 200μs, and the current to 1 mA
__42. Set up microelectrodes to isolated stimulator
__43. Use clay to hold leads at the base of the electrodes in place
__44. Position the electrodes w/ the tips resting on the surface of the gracilis anterior midway between the saphenous and profunda
__45. Turn on the stimulator and start stimulation
__46. Adjust electrode placement and current for a maximal localized contraction, then stop stimulation
__47. Apply PBS to tissue, cover preparation with plastic wrap for entire duration, and equilibrate for 30 minutes to regain resting vascular tone

__48. Repeat the surgical exposure, equilibrate, complete electrode test and FVD procedures on control limb

**Functional Vasodilation**

__49. Change the frequency to 8 Hz (125 ms pulse interval)

__50. Switch on the trans-illuminator and place clay to block light from eyes

__51. Open QCapturePro and position the intravital microscope above the collateral arteriole

__52. Acquire resting images of the arteriole in the Midzone (if possible: Reentry and Stem)

__53. Stimulate the muscle for 90 seconds

__54. Capture images of collateral immediately after simulation (series of 10), save all images acquired (if possible: reentry, stem)

__55. Remove plastic wrap and maximally dilate by applying SNP, cover with plastic wrap again

__56. Capture images at point of maximum dilation (max wait time is 5 minutes), save all images acquired (if possible: reentry, stem)

__57. Remove plastic wrap and rinse muscle with PBS

__58. Maximally constrict with NE, cover with plastic wrap again

__59. Capture images at point of maximum constriction (max wait time is 5 minutes), save all images acquired (if possible: reentry, stem)

**Post-Surgical**

__60. Blunt dissect gracilis anterior to be able to resect

__61. Pass to perfusion fixer or perform cervical dislocation to euthanize animal

__62. Turn off isofluorane, flow, and close oxygen

__63. Wash all instruments used during procedure

__64. Wipe down the surgical area with IPA

**Perfusion Fixation, Microfil Vascular Casting, and Dissection Protocol**

Date _____

Mouse Information

DOB: _____

Sex: _____

Genotype/strain: _____

Cage: _____

Weight (g): _____

**Materials**

Non-Sterile Instruments

___ 1. Standard Pattern Forceps (1)

___ 2. Bone Scissors (1)

___ 3. Iris Scissors (1)

___ 4. Hemostats (1)

___ 5. Microdissection Scissors (1)

___ 6. Vascular Clamp (1)

Obtained in surgery site

___ 7. Tape

___ 8. 20 mL Syringe (1)

___ 9. 10 mL Syringes (2)

___ 10. Bench cover

___ 11. Heating pad

___ 12. Catheter with PE-100 tubing

___ 13. Tubing with stopcock

___ 14. Isoflurane Anesthetic

___ 15. 2x2 & 4x4 Gauze sponges

___ 16. Silk suture

___ 17. Syringe pump

**Vasodilator Cocktail Preparation**

___ 18. Turn on water bath to 37°C

___ 19. 400 µL Heparin

___ 20. 1 mL Sodium Nitroprusside (SNP) (orange)

___ 21. 600 µL Adenosine (clear)

___ 22. 38 mL PBS solution

___ 23. Thaw SNP and Adenosine

___ 24. Add heparin, SNP, Adenosine, and PBS solution in a 50 mL conical

___ 25. Place vasodilator cocktail in water bath

**Microfil Cocktail Preparation**

___ 26. 2 mL Microfil MV-120

___ 27. 1.5 mL Microfil HV-Diluent

___ 28. 1.25 mL Microfil MV-Diluent

___ 29. Add MV-122, HV-Diluent, and MV-Diluent into a 15 mL conical, vortex, and place in bath

**Procedure Preparation**

___ 30. Weigh animal

___ 31. Obtain saline filled petri-dish, cotton swab, and instruments

**Fixation**

___ 32. If not already anesthetized, anesthetize mouse with Isoflurane

___ 33. Tape all 4 limbs to a gauze sponge over the heating pad in the supine position such that its nose is in the nose cone

___ 34. Insert rectal temperature probe and turn on heating pad

___ 35. Loosely tie a tourniquet around both ankles

___ 36. Fill the 20 mL syringe with 20mL of the vasodilator cocktail, attach the tubing with a stopcock, and place in the syringe pump

___ 37. Using standard pattern forceps and iris scissors, tent the skin below the sternum and cut laterally

___ 38. Cut both sides of the skin up to the clavicle such that the incision is in a U shape

___ 39. Blunt dissect the connective tissue away between the skin and ribcage

___ 40. Using bone scissors and forceps, cut the ribcage up to the clavicle, cut laterally across the diaphragm, and cut the other side of the ribcage up to the clavicle

___ 41. Clamp the ribcage at the sternum with the hemostats and reflect it over the head

___ 42. Tear connective tissue around the heart, insert needle into the apex of the heart, and cut the right atrium

___ 43. Inject vasodilator cocktail at 5mL/min with syringe pump until the saphenous vein clears and soak excess blood with 4x4 gauze

___ 44. Inject 5mL of 4% PFA at 4mL/min

___ 45. Add 0.2 mL of curing agent to Microfil cocktail

___ 46. Draw up Microfil cocktail in 10 mL syringe and attach the catheter and tubing

___ 47. Make a small incision in the apex of the heart, insert catheter, and clamp with vascular clamp

___ 48. Inject 2 mL of Microfil cocktail at 0.5mL/min

___ 49. Once Microfil has passed the knee, pause the Microfil and tie the tourniquets around both ankles tightly. Resume Microfil until satisfied

___ 50. After letting the mouse sit for 5 minutes, remove mouse from heat pad and take out catheter while leaving vascular clamp

___ 51. Place mouse in bag (cover open wounds with saran wrap) and let sit overnight in fridge

___ 52. Cover scope, turn off water bath, turn off oxygen and Isoflurane, clean instruments

# One-way ANOVA: Fold Increase versus bFGF Dose

## Method

| | |
|---|---|
| Null hypothesis | All means are equal |
| Alternative hypothesis | Not all means are equal |
| Significance level | α = 0.05 |

*Equal variances were assumed for the analysis.*

## Factor Information

| Factor | Levels | Values |
|---|---|---|
| bFGF Dose | 5 | 0.5X, 0X, 1X, 2X, N/A |

## Analysis of Variance

| Source | DF | Seq SS | Contribution | Adj SS | Adj MS | F-Value | P-Value |
|---|---|---|---|---|---|---|---|
| bFGF Dose | 4 | 28.579 | 82.48% | 28.579 | 7.1447 | 11.77 | 0.001 |
| Error | 10 | 6.069 | 17.52% | 6.069 | 0.6069 | | |
| Total | 14 | 34.648 | 100.00% | | | | |

## Model Summary

| S | R-sq | R-sq(adj) | PRESS | R-sq(pred) |
|---|---|---|---|---|
| 0.779066 | 82.48% | 75.48% | 13.6563 | 60.59% |

## Means

| bFGF Dose | N | Mean | StDev | 95% CI |
|---|---|---|---|---|
| 0.5X | 3 | 4.167 | 0.601 | (3.164, 5.169) |
| 0X | 3 | 3.361 | 0.625 | (2.359, 4.363) |
| 1X | 3 | 5.972 | 0.867 | (4.970, 6.974) |
| 2X | 3 | 6.833 | 1.127 | (5.831, 7.836) |
| N/A | 3 | 3.556 | 0.509 | (2.553, 4.558) |

*Pooled StDev = 0.779066*

## Tukey Pairwise Comparisons

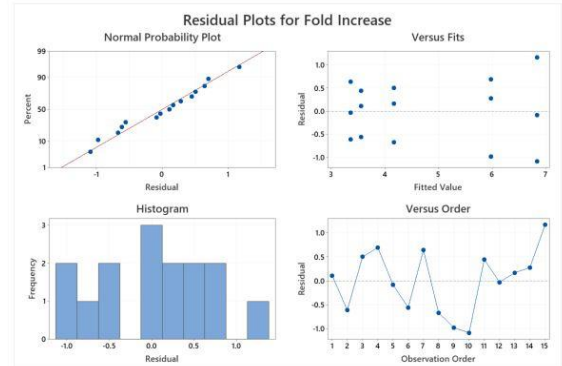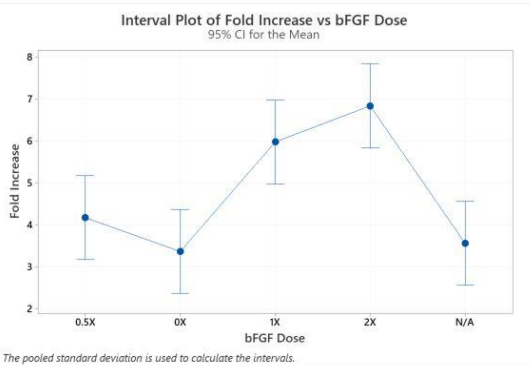### Grouping Information Using the Tukey Method and 95% Confidence

| bFGF Dose | N | Mean | Grouping | | |
|---|---|---|---|---|---|
| 2X | 3 | 6.833 | A | | |
| 1X | 3 | 5.972 | A | B | |
| 0.5X | 3 | 4.167 | | B | C |
| N/A | 3 | 3.556 | | | C |
| 0X | 3 | 3.361 | | | C |

*Means that do not share a letter are significantly different.*

### Tukey Simultaneous Tests for Differences of Means

| Difference of Levels | Difference of Means | SE of Difference | 95% CI | T-Value | Adjusted P-Value |
|---|---|---|---|---|---|
| 0X - 0.5X | -0.806 | 0.636 | (-2.897, 1.286) | -1.27 | 0.716 |
| 1X - 0.5X | 1.806 | 0.636 | (-0.286, 3.897) | 2.84 | 0.100 |
| 2X - 0.5X | 2.667 | 0.636 | (0.575, 4.758) | 4.19 | 0.012 |
| N/A - 0.5X | -0.611 | 0.636 | (-2.703, 1.480) | -0.96 | 0.866 |
| 1X - 0X | 2.611 | 0.636 | (0.520, 4.703) | 4.10 | 0.014 |
| 2X - 0X | 3.472 | 0.636 | (1.381, 5.564) | 5.46 | 0.002 |
| N/A - 0X | 0.194 | 0.636 | (-1.897, 2.286) | 0.31 | 0.998 |
| 2X - 1X | 0.861 | 0.636 | (-1.230, 2.953) | 1.35 | 0.667 |
| N/A - 1X | -2.417 | 0.636 | (-4.508, -0.325) | -3.80 | 0.023 |
| N/A - 2X | -3.278 | 0.636 | (-5.369, -1.186) | -5.15 | 0.003 |

*Individual confidence level = 99.18%*

Tukey Simultaneous 95% CIs
Differences of Means for Fold Increase



Interval Plot of Fold Increase vs bFGF Dose
95% CI for the Mean

The pooled standard deviation is used to calculate the intervals.



Residual Plots for Fold Increase
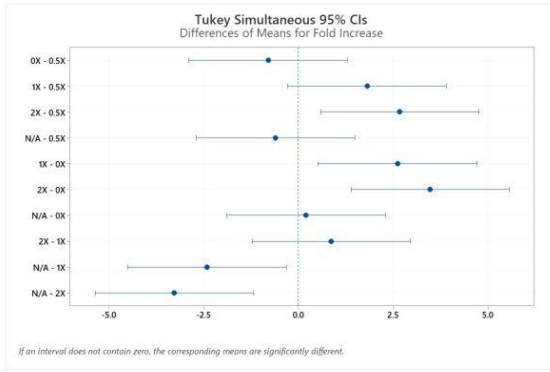
# One-way ANOVA: Fold Increase versus P38 Dose

## Method

| | |
|---|---|
| Null hypothesis | All means are equal |
| Alternative hypothesis | Not all means are equal |
| Significance level | α = 0.05 |

*Equal variances were assumed for the analysis.*

## Factor Information

| Factor | Levels | Values |
|---|---|---|
| P38 Dose | 5 | 0.5X, 0X, 1X, 2X, N/A |

## Analysis of Variance

| Source | DF | Seq SS | Contribution | Adj SS | Adj MS | F-Value | P-Value |
|---|---|---|---|---|---|---|---|
| P38 Dose | 4 | 22.115 | 85.44% | 22.115 | 5.5289 | 14.67 | 0.000 |
| Error | 10 | 3.768 | 14.56% | 3.768 | 0.3768 | | |
| Total | 14 | 25.884 | 100.00% | | | | |

## Model Summary

| S | R-sq | R-sq(adj) | PRESS | R-sq(pred) |
|---|---|---|---|---|
| 0.613868 | 85.44% | 79.62% | 8.47875 | 67.24% |

## Means

| P38 Dose | N | Mean | StDev | 95% CI |
|---|---|---|---|---|
| 0.5X | 3 | 5.400 | 0.529 | (4.610, 6.190) |
| 0X | 3 | 6.333 | 0.577 | (5.544, 7.123) |
| 1X | 3 | 5.972 | 0.867 | (5.183, 6.762) |
| 2X | 3 | 3.444 | 0.509 | (2.655, 4.234) |
| N/A | 3 | 3.556 | 0.509 | (2.766, 4.345) |

*Pooled StDev = 0.613868*

## Tukey Pairwise Comparisons

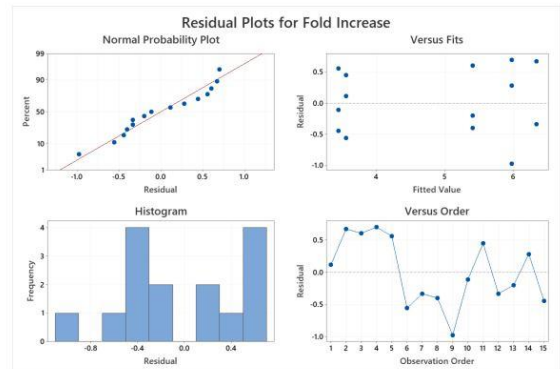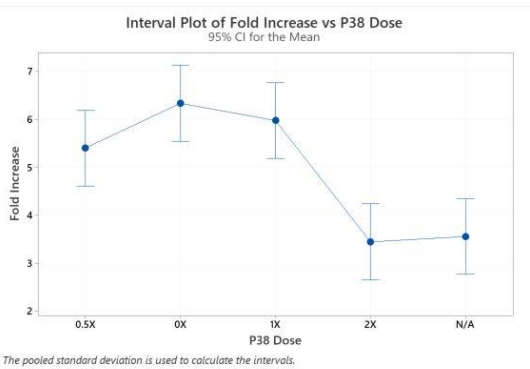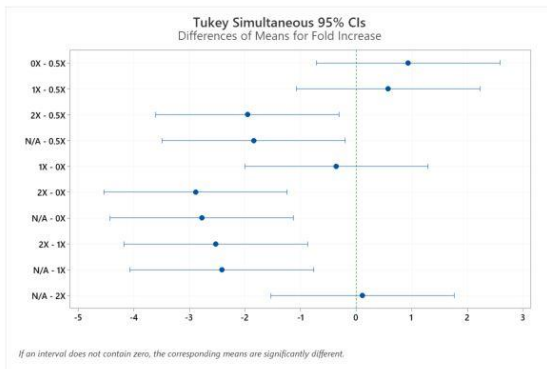### Grouping Information Using the Tukey Method and 95% Confidence

| P38 Dose | N | Mean | Grouping | |
|---|---|---|---|---|
| 0X | 3 | 6.333 | A | |
| 1X | 3 | 5.972 | A | |
| 0.5X | 3 | 5.400 | A | |
| N/A | 3 | 3.556 | | B |
| 2X | 3 | 3.444 | | B |

*Means that do not share a letter are significantly different.*

### Tukey Simultaneous Tests for Differences of Means

| Difference of Levels | Difference of Means | SE of Difference | 95% CI | T-Value | Adjusted P-Value |
|---|---|---|---|---|---|
| 0X - 0.5X | 0.933 | 0.501 | (-0.715, 2.581) | 1.86 | 0.394 |
| 1X - 0.5X | 0.572 | 0.501 | (-1.076, 2.220) | 1.14 | 0.782 |
| 2X - 0.5X | -1.956 | 0.501 | (-3.604, -0.308) | -3.90 | 0.019 |
| N/A - 0.5X | -1.844 | 0.501 | (-3.492, -0.196) | -3.68 | 0.027 |
| 1X - 0X | -0.361 | 0.501 | (-2.009, 1.287) | -0.72 | 0.947 |
| 2X - 0X | -2.889 | 0.501 | (-4.537, -1.241) | -5.76 | 0.001 |
| N/A - 0X | -2.778 | 0.501 | (-4.426, -1.130) | -5.54 | 0.002 |
| 2X - 1X | -2.528 | 0.501 | (-4.176, -0.880) | -5.04 | 0.004 |
| N/A - 1X | -2.417 | 0.501 | (-4.065, -0.769) | -4.82 | 0.005 |
| N/A - 2X | 0.111 | 0.501 | (-1.537, 1.759) | 0.22 | 0.999 |

*Individual confidence level = 99.18%*



Tukey Simultaneous 95% CIs
Differences of Means for Fold Increase

*If an interval does not contain zero, the corresponding means are significantly different.*



Interval Plot of Fold Increase vs P38 Dose
95% CI for the Mean

*The pooled standard deviation is used to calculate the intervals.*



Residual Plots for Fold Increase

# One-way ANOVA: Cell Number (10^6) versus Supplementation

## Method

| | |
|---|---|
| Null hypothesis | All means are equal |
| Alternative hypothesis | Not all means are equal |
| Significance level | $\alpha = 0.05$ |

*Equal variances were assumed for the analysis.*

## Factor Information

| Factor | Levels | Values |
|---|---|---|
| Supplementation | 4 | -/-, -/+, +/-, +/+ |

## Analysis of Variance

| Source | DF | Seq SS | Contribution | Adj SS | Adj MS | F-Value | P-Value |
|---|---|---|---|---|---|---|---|
| Supplementation | 3 | 1.1703 | 91.32% | 1.1703 | 0.390104 | 70.13 | 0.000 |
| Error | 20 | 0.1112 | 8.68% | 0.1112 | 0.005562 | | |
| Total | 23 | 1.2816 | 100.00% | | | | |

## Model Summary

| S | R-sq | R-sq(adj) | PRESS | R-sq(pred) |
|---|---|---|---|---|
| 0.0745822 | 91.32% | 90.02% | 0.1602 | 87.50% |

## Means

| Supplementation | N | Mean | StDev | 95% CI |
|---|---|---|---|---|
| -/- | 6 | 0.4250 | 0.0524 | (0.3615, 0.4885) |
| -/+ | 6 | 0.5333 | 0.0606 | (0.4698, 0.5968) |
| +/- | 6 | 0.8583 | 0.0736 | (0.7948, 0.9218) |
| +/+ | 6 | 0.9583 | 0.1021 | (0.8948, 1.0218) |

*Pooled StDev = 0.0745822*

## Tukey Pairwise Comparisons

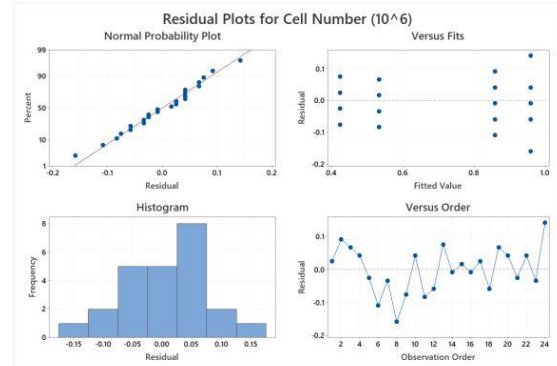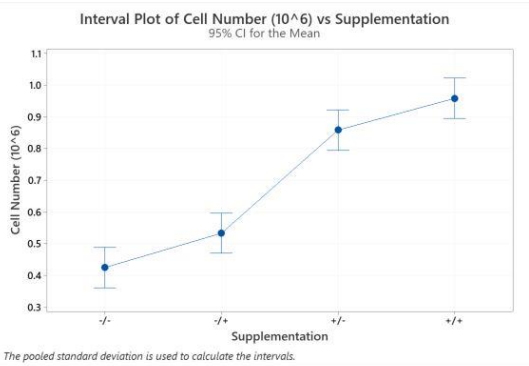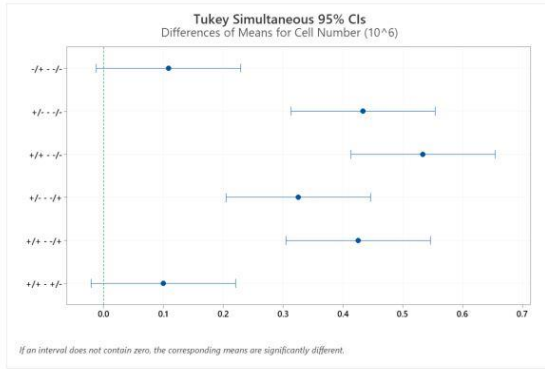### Grouping Information Using the Tukey Method and 95% Confidence

| Supplementation | N | Mean | Grouping | |
|---|---|---|---|---|
| +/+ | 6 | 0.9583 | A | |
| +/- | 6 | 0.8583 | A | |
| -/+ | 6 | 0.5333 | | B |
| -/- | 6 | 0.4250 | | B |

*Means that do not share a letter are significantly different.*

### Tukey Simultaneous Tests for Differences of Means

| Difference of Levels | Difference of Means | SE of Difference | 95% CI | T-Value | Adjusted P-Value |
|---|---|---|---|---|---|
| -/+ - -/- | 0.1083 | 0.0431 | (-0.0122, 0.2289) | 2.52 | 0.088 |
| +/- - -/- | 0.4333 | 0.0431 | (0.3128, 0.5539) | 10.06 | 0.000 |
| +/+ - -/- | 0.5333 | 0.0431 | (0.4128, 0.6539) | 12.39 | 0.000 |
| +/- - -/+ | 0.3250 | 0.0431 | (0.2044, 0.4456) | 7.55 | 0.000 |
| +/+ - -/+ | 0.4250 | 0.0431 | (0.3044, 0.5456) | 9.87 | 0.000 |
| +/+ - +/- | 0.1000 | 0.0431 | (-0.0206, 0.2206) | 2.32 | 0.126 |

*Individual confidence level = 98.89%*

Tukey Simultaneous 95% CIs
Differences of Means for Cell Number (10^6)

If an interval does not contain zero, the corresponding means are significantly different.



Interval Plot of Cell Number (10^6) vs Supplementation
95% CI for the Mean

The pooled standard deviation is used to calculate the intervals.



Residual Plots for Cell Number (10^6)

## One-way ANOVA: % MyoD Positive versus Supplementation

### Method

| Null hypothesis | All means are equal |
|---|---|
| Alternative hypothesis | Not all means are equal |
| Significance level | $\alpha = 0.05$ |

*Equal variances were assumed for the analysis.*

### Factor Information

| Factor | Levels | Values |
|---|---|---|
| Supplementation | 4 | -/-, -/+, +/-, +/+ |

### Analysis of Variance

| Source | DF | Seq SS | Contribution | Adj SS | Adj MS | F-Value | P-Value |
|---|---|---|---|---|---|---|---|
| Supplementation | 3 | 684.9 | 74.35% | 684.9 | 228.29 | 7.73 | 0.009 |
| Error | 8 | 236.3 | 25.65% | 236.3 | 29.54 | | |
| Total | 11 | 921.2 | 100.00% | | | | |

### Model Summary

| S | R-sq | R-sq(adj) | PRESS | R-sq(pred) |
|---|---|---|---|---|
| 5.43479 | 74.35% | 64.73% | 531.664 | 42.28% |

### Means

| Supplementation | N | Mean | StDev | 95% CI |
|---|---|---|---|---|
| -/- | 3 | 81.13 | 7.86 | (73.89, 88.37) |
| -/+ | 3 | 99.225 | 1.343 | (91.989, 106.461) |
| +/- | 3 | 92.86 | 7.39 | (85.62, 100.10) |
| +/+ | 3 | 100.0 | 0.0 | (92.8, 107.2) |

*Pooled StDev = 5.43479*

68

## Tukey Pairwise Comparisons

### Grouping Information Using the Tukey Method and 95% Confidence

| Supplementation | N | Mean | Grouping | |
|---|---|---|---|---|
| +/+ | 3 | 100.0 | A | |
| -/+ | 3 | 99.225 | A | |
| +/- | 3 | 92.86 | A | B |
| -/- | 3 | 81.13 | | B |

*Means that do not share a letter are significantly different.*

### Tukey Simultaneous Tests for Differences of Means

| Difference of Levels | Difference of Means | SE of Difference | 95% CI | T-Value | Adjusted P-Value |
|---|---|---|---|---|---|
| -/+ - -/- | 18.09 | 4.44 | (3.88, 32.31) | 4.08 | 0.015 |
| +/- - -/- | 11.73 | 4.44 | (-2.48, 25.94) | 2.64 | 0.110 |
| +/+ - -/- | 18.87 | 4.44 | (4.66, 33.08) | 4.25 | 0.012 |
| +/- - -/+ | -6.37 | 4.44 | (-20.58, 7.85) | -1.43 | 0.514 |
| +/+ - -/+ | 0.78 | 4.44 | (-13.44, 14.99) | 0.17 | 0.998 |
| +/+ - +/- | 7.14 | 4.44 | (-7.07, 21.35) | 1.61 | 0.426 |

*Individual confidence level = 98.74%*
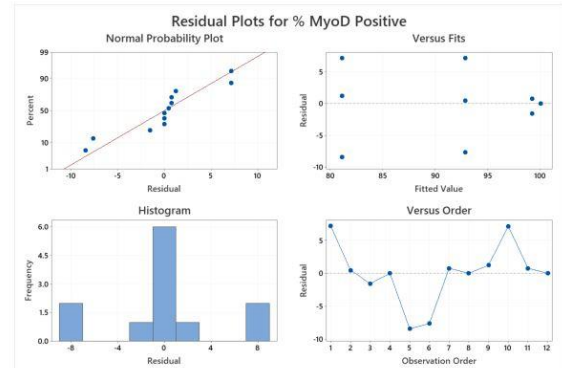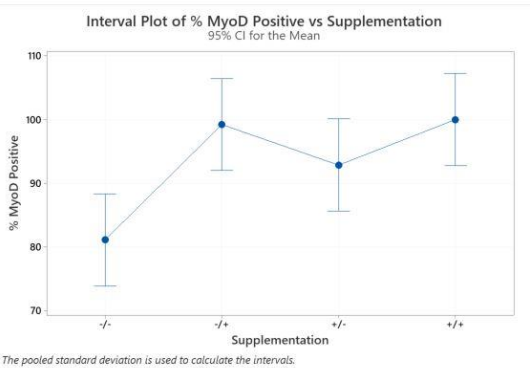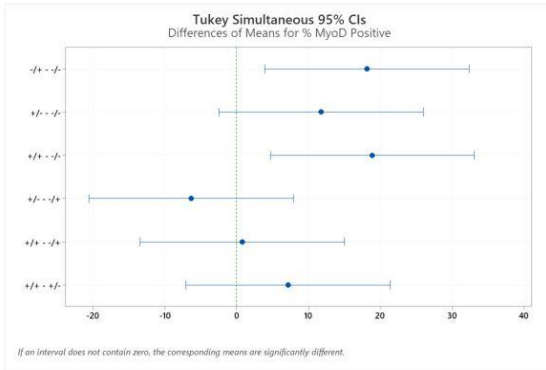
# One-way ANOVA: % PAX7 Positive versus Supplementation

## Method

| | |
|---|---|
| Null hypothesis | All means are equal |
| Alternative hypothesis | Not all means are equal |
| Significance level | α = 0.05 |

*Equal variances were assumed for the analysis.*

## Factor Information

| Factor | Levels | Values |
|---|---|---|
| Supplementation | 4 | -/-, -/+, +/-, +/+ |

## Analysis of Variance

| Source | DF | Seq SS | Contribution | Adj SS | Adj MS | F-Value | P-Value |
|---|---|---|---|---|---|---|---|
| Supplementation | 3 | 450.2 | 55.51% | 450.2 | 150.08 | 3.33 | 0.077 |
| Error | 8 | 360.9 | 44.49% | 360.9 | 45.11 | | |
| Total | 11 | 811.1 | 100.00% | | | | |

## Model Summary

| S | R-sq | R-sq(adj) | PRESS | R-sq(pred) |
|---|---|---|---|---|
| 6.71651 | 55.51% | 38.82% | 812.008 | 0.00% |

## Means

| Supplementation | N | Mean | StDev | 95% CI |
|---|---|---|---|---|
| -/- | 3 | 84.62 | 13.03 | (75.68, 93.57) |
| -/+ | 3 | 99.225 | 1.343 | (90.283, 108.167) |
| +/- | 3 | 94.46 | 2.96 | (85.52, 103.40) |
| +/+ | 3 | 100.0 | 0.0 | (91.1, 108.9) |

*Pooled StDev = 6.71651*

## Tukey Pairwise Comparisons

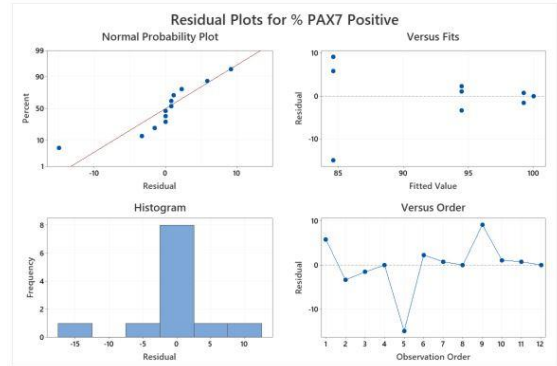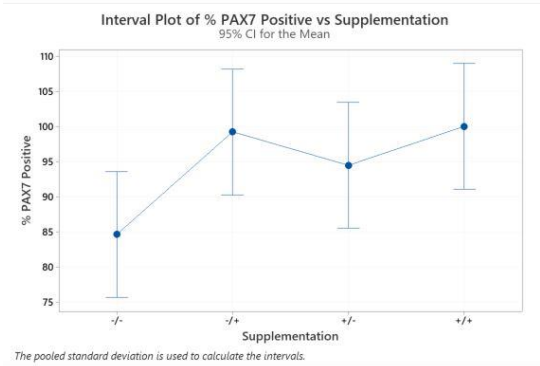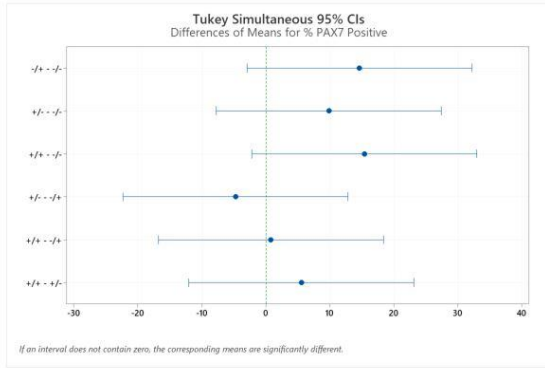### Grouping Information Using the Tukey Method and 95% Confidence

| Supplementation | N | Mean | Grouping |
|---|---|---|---|
| +/+ | 3 | 100.0 | A |
| -/+ | 3 | 99.225 | A |
| +/- | 3 | 94.46 | A |
| -/- | 3 | 84.62 | A |

*Means that do not share a letter are significantly different.*

### Tukey Simultaneous Tests for Differences of Means

| Difference of Levels | Difference of Means | SE of Difference | 95% CI | T-Value | Adjusted P-Value |
|---|---|---|---|---|---|
| -/+ - -/- | 14.60 | 5.48 | (-2.97, 32.17) | 2.66 | 0.107 |
| +/- - -/- | 9.84 | 5.48 | (-7.73, 27.40) | 1.79 | 0.342 |
| +/+ - -/- | 15.38 | 5.48 | (-2.19, 32.94) | 2.80 | 0.088 |
| +/- - -/+ | -4.76 | 5.48 | (-22.33, 12.80) | -0.87 | 0.821 |
| +/+ - -/+ | 0.78 | 5.48 | (-16.79, 18.34) | 0.14 | 0.999 |
| +/+ - +/- | 5.54 | 5.48 | (-12.03, 23.10) | 1.01 | 0.749 |

*Individual confidence level = 98.74%*

Tukey Simultaneous 95% CIs
Differences of Means for % PAX7 Positive

If an interval does not contain zero, the corresponding means are significantly different.



Interval Plot of % PAX7 Positive vs Supplementation
95% CI for the Mean

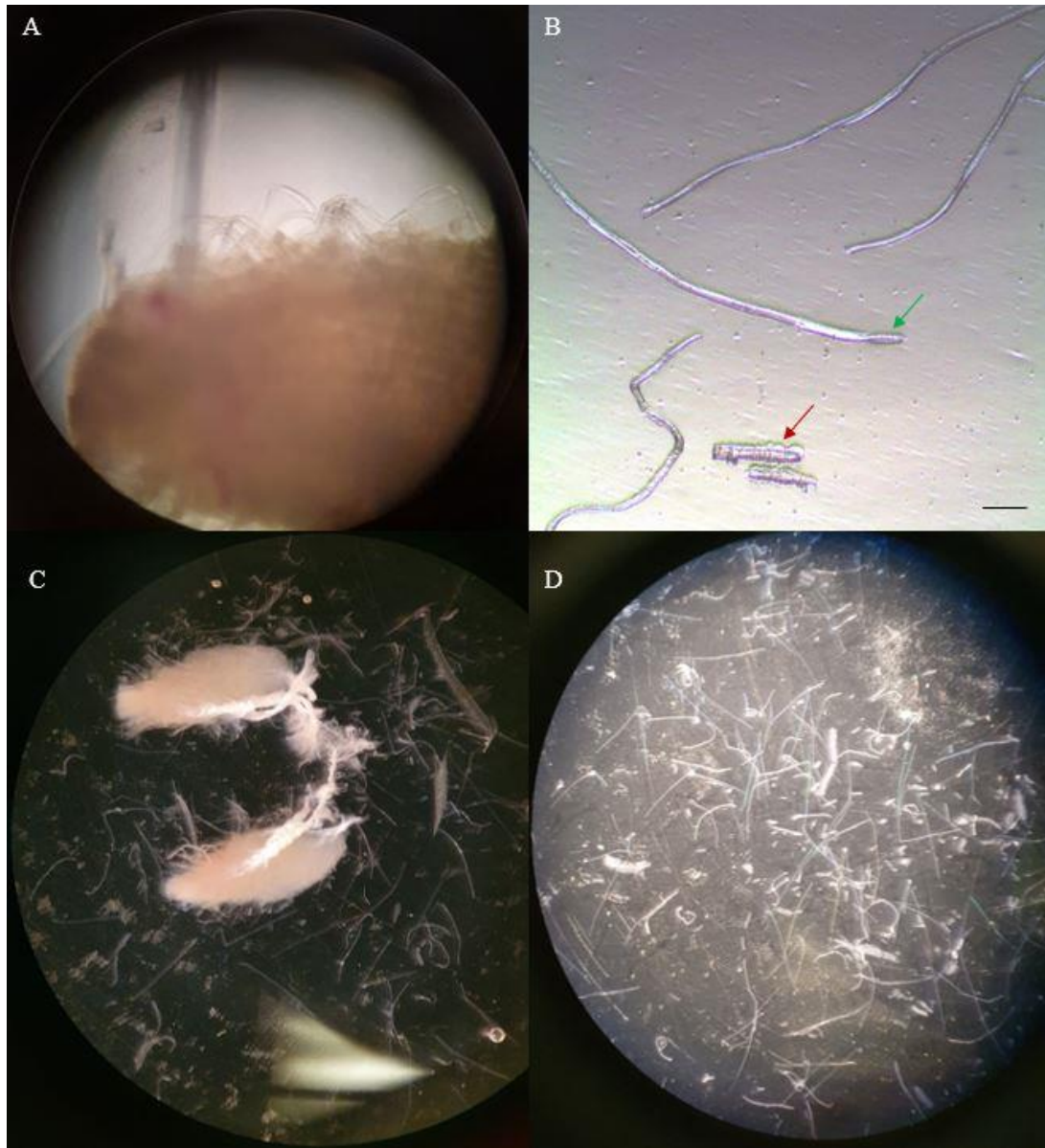The pooled standard deviation is used to calculate the intervals.



Residual Plots for % PAX7 Positive

Figure S1: Myofiber Isolation Process. A, Myofibers begin to protrude out of muscle body following enzymatic digestion. B, Viable (green arrow) and hypercontracted (red arrow) myofibers. C, Mechanical separation of myofibers from muscle body. D, Myofibers prior to separation and introduction into culture flask.
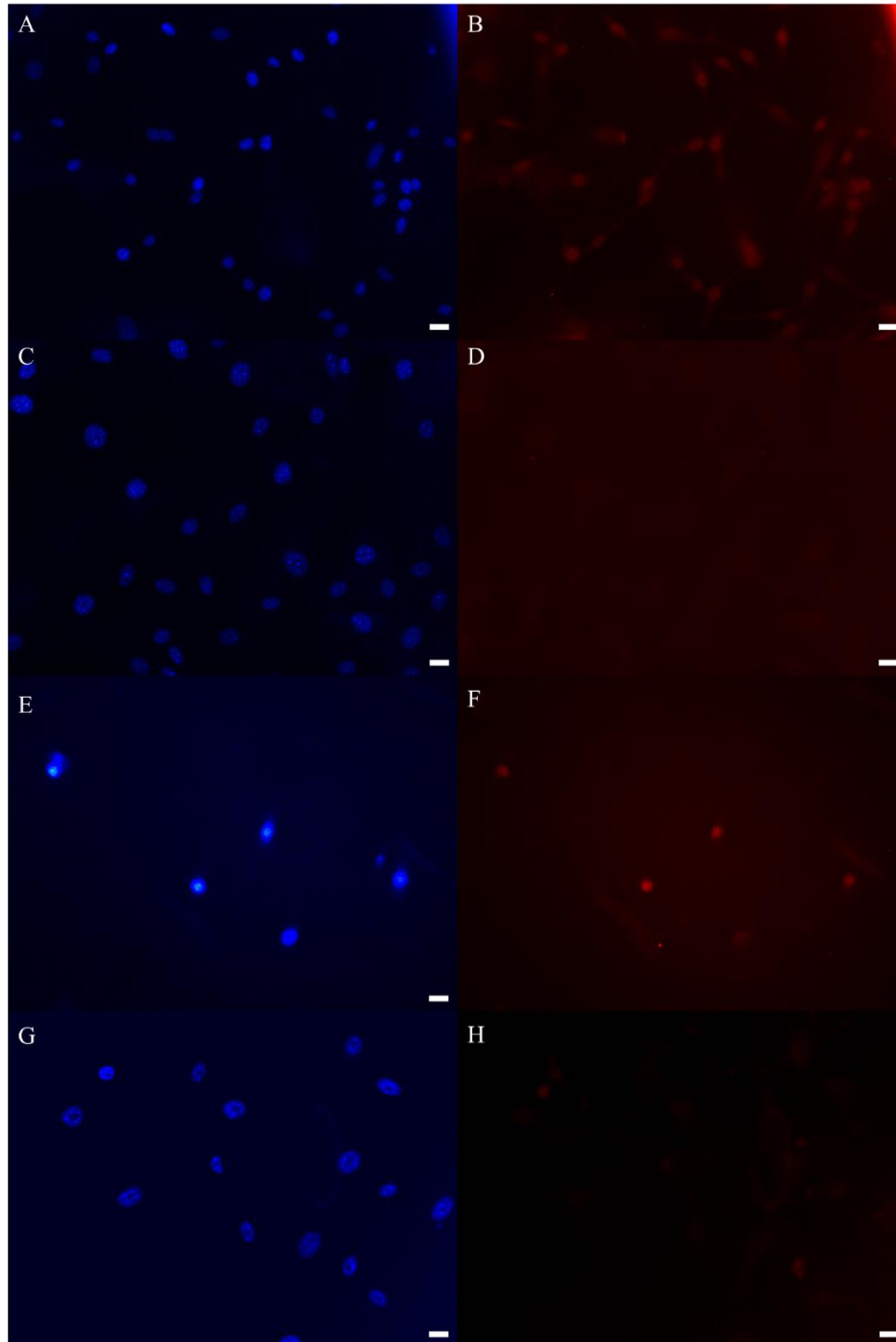
Figure S2: Sample Control Stain. A, B, Myoblasts labeled using DAPI nuclear stain (A) and Pax7 (B). C, D, Fibroblasts (NIH-3T3) labeled using DAPI nuclear stain (A) and Pax7 (B). Fibroblasts stained negative for Pax7, confirming the selectivity of the antibody and validity of the immunostaining protocol. E, F Myoblasts cultured on gelatin labeled using DAPI nuclear stain (E) and Pax7 (F). G, H, Fibroblasts cultured on gelatin (NIH-3T3) labeled using DAPI nuclear stain (G) and Pax7 (H). Fibroblasts stained negative for Pax7, confirming the selectivity of the antibody (Scale bars: 20µm)
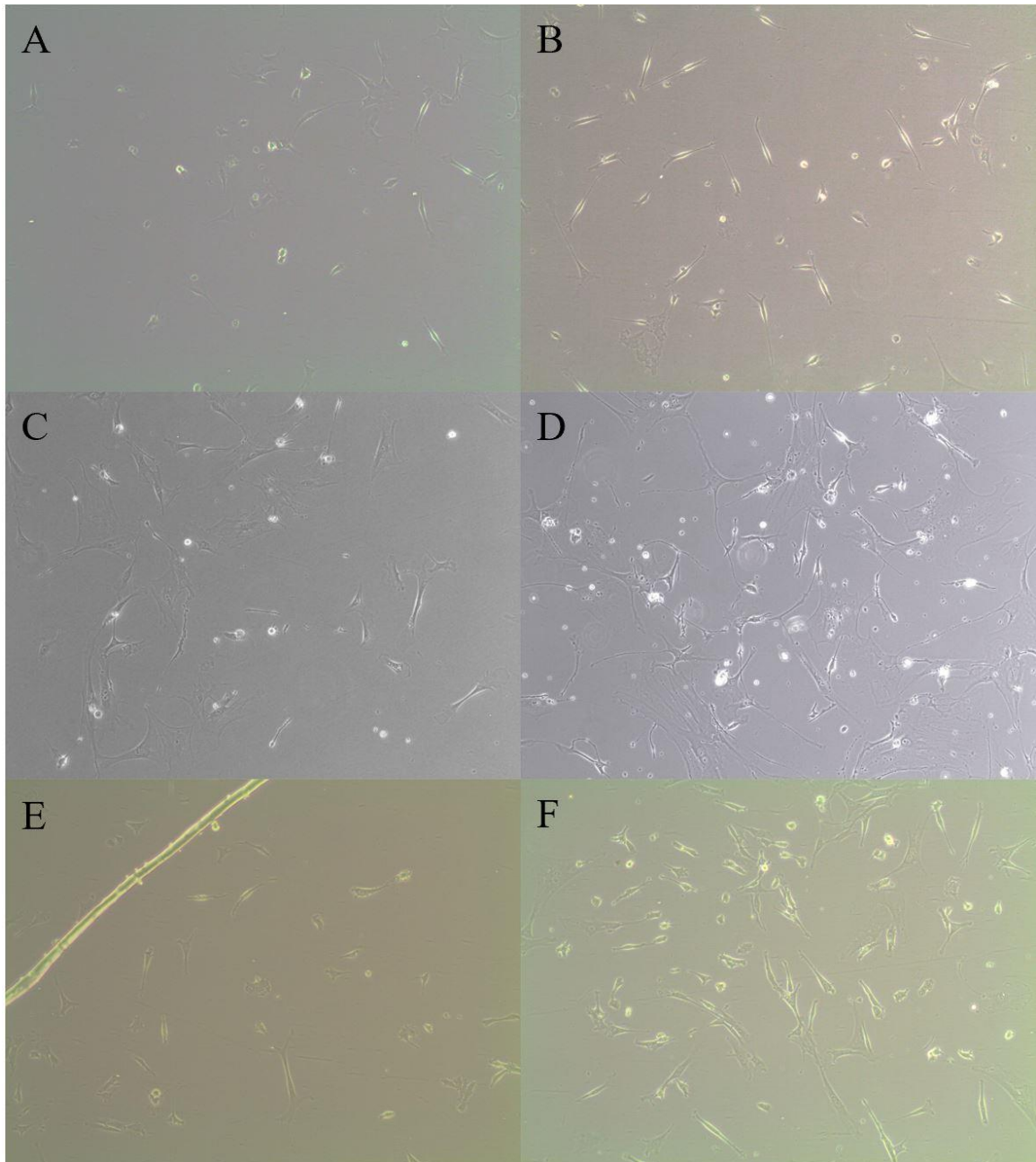
Figure S3: Common Morphology of Myogenic Cells During Troubleshooting. A, B, Day 3 (A) and day 7 (B) myoblasts in culture without (or expired) bFGF supplementation. C, D, Day 3 (C) and day 7 (D) myoblasts in culture without SB 203580 supplementation. E, F, Day 3 (E) and day 7 (F) myoblasts in culture supplemented with expired (defective) SB 203580.